Professional report of the NKFIH PD 132851 grant

Endothelial dysfunction in the early stage of atherosclerosis: a potential role of autotaxin

Endothelial dysfunction refers to the complex structural and functional alteration of the endothelium that manifests in several cardiovascular diseases including atherosclerosis, diabetes, and hypertension. It is characterized by endothelial cell activation resulting in increased adhesion molecule and cytokine expression and impaired endothelial permeability. The hallmark of endothelial dysfunction is the altered endothelium-dependent vasodilation, mostly attributed to the disrupted synthesis and reduced bioavailability of nitric oxide (NO) (1).

Autotaxin (ATX; or ENPP2) is one of seven mammalian ectonucleotide pyrophosphatases/phosphodiesterases (ENPPs), which hydrolyze pyrophosphate or phosphodiester bonds in a range of extracellular molecules. ATX is unique among the ENPPs, in that it functions as a lysophospholipase D (lysoPLD), generating the signaling phospholipid lysophosphatidic acid (LPA) from lysophosphatidylcholine (LPC), an abundant plasma phospholipid (2). LPA is a potent extracellular signaling molecule with multiple physiological actions, and signals through six distinct G protein-coupled receptors (termed LPA1–6) expressed by many different cell types (3).

The main aim of this research grant was to to investigate the potential role of the LPC-ATX-LPA axis in the development of the initial step of atherosclerosis: endothelial dysfunction. We hypothesized that increased expression and/or activity of ATX in the vascular wall and consequent conversion of LPC to LPA may contribute to abnormalities in the production and/or bioavailability of endothelium-derived NO and resultant deleterious changes in vascular reactivity and functions. The first part of this plan was to rule out the possible involvement of ATX in the development of endothelial dysfunction elicited by LPC.

1.1 Autotaxin-Lysophosphatidic Acid Receptor 5 Axis Evokes Endothelial Dysfunction via Reactive Oxygen Species Signaling

Endothelial dysfunction refers to abnormalities in the production and bioavailability of endothelium-derived NO and resultant deleterious changes in vascular reactivity. To test NO mediated relaxation, we investigated dose-response relationship of acetylcholine (ACh) in phenylephrine precontracted isolated thoracic aorta segments before and after treatment with LPC by wire myography. We observed that in LPC treated WT vessels, the ACh-induced vasorelaxant responses were markedly attenuated. To investigate the contribution of ATX to this deleterious effect of LPC, vessels were pre-treated with the selective ATX inhibitor GLPG1690. GLPG1690 significantly decreased the LPC-induced endothelial dysfunction, suggesting the involvement of ATX in the effect of LPC.

Thereafter we examined whether ATX's product, LPA also contributes to the effect. Therefore, the effect of LPC was tested on aorta segments isolated from mice KO for different LPA receptors. In the case of *Lpar1*, *Lpar2* and *Lpar4* KO, the effect of LPC was similar to that observed in WT mice. On the contrary, the impairment of ACh-induced vasorelaxation by LPC was markedly attenuated in $Lpar_5$ KO mice. These results indicate that LPC-derived LPA may contribute to the development of endothelial dysfunction through LPA_5 receptor activation. Additionally, we also examined the LPA receptor and ATX expression profile in aortic tissue isolated from WT and *Lpar5* KO mice using quantitative real-time PCR. Our data showed that *Lpar5* deletion did not significantly affect the expression of LPA_1, LPA_2, LPA_3, LPA_4, LPA_6 receptors and ATX as no significant differences in mRNA expression rate were detected relative to WT.

In the next phase of the study, we investigated the downstream signaling mechanism involved in the LPA receptor-mediated portion of the LPC-induced endothelial dysfunction. Considering that superoxide is a well-known factor participating in the development of endothelial dysfunction (1), we tested the effect of SOD on the deleterious effect of LPC. SOD prevented the effect of LPC treatment in WT vessels. Interestingly, this beneficial effect of SOD was absent in *Lpar5* KO vessels, indicating that LPA_5 receptor activation drives ROS production.

To confirm the involvement of LPA_5 receptor in ROS generation upon LPC treatment, H_2O_2 production assay was performed in the vessels. LPC induced a marked increase in extracellular H_2O_2 levels in aortic tissue isolated from WT mice, however, its effect was

significantly diminished in *Lpar5* KO vessels. These data suggest that the LPA_5 activation is involved in LPC-evoked ROS production.

In conclusion, we have shown that the development of LPC-induced impairment of endothelium-dependent vasorelaxation requires the conversion of LPC to LPA by the ATX enzyme in mouse aortic tissue. This locally formed LPA appears to activate LPA_5 receptor, triggering signaling pathways that lead to an elevated production of ROS and subsequent endothelial dysfunction. We have prepared and submitted a manuscript containing these results which is currently under peer review and can be found attached to this report.

According to the research plan, the other goal of the project was to rule out the involvement of ATX in the development of atherosclerosis related endothelial dysfunction. First, we tried to set a mouse model, in which endothelial dysfunction is present in the thoracic aorta, as an early sign of atherogenesis. ApoE mice were given 'Western-type' diet for 12 weeks, and every second week, 2 mice were sacrificed to test endothelium dependent relaxation of the aorta. Unfortunately, neither ACh induced vasorelaxation, nor its nitric oxide dependency decreased during the investigated period. We have also unsuccessfully tested LDL receptor KO mice, as they are widely used as another model of accelerated atherogenesis. On the other hand, atherosclerotic plaque formation was clearly detectable with Oil Red staining in both animal models.

After these disappointing result we moved to other disease models where the role of ATX in vascular processes can be suspected. One such is the endothelial dysfunction present in vascular inflammation. According to a recent publication, aortic expression of ATX increases in vasculitis (4). We induced vasculitis with two different methods: angiotensin II was applied for two weeks via osmotic minipump, or lipopolysaccharide was injected 12 hours before the experiments. The effect of LPC in the aorta of the treated animals was significantly, but only moderately bigger than in the controls. Also, the slightly increased effect of LPC was detectable in *Lpar5* KO animals as well, suggesting the involvement of another LPA receptor in the process.

We have also started to investigate endothelial dysfunction present in diabetes mellitus. A well known mouse model of type 2 diabetes (T2DM), the leptin receptor deficient db/db mice develop endothelial dysfunction in the thoracic aorta (5). We have found, that the plasma level of LPC, measured by HPLC-MS/MS is elevated in db/db diabetic mice.

Furthermore, ATX showed higher expression levels in the subcutaneous and periaortic adipose tissue of the diabetic mice compared to control measured by qPCR. According to literature data, the majority of plasma ATX is originated from adipose cells (6), and ATX can attach to the surface of endothelial cells through activated integrin receptors and produce LPA in the proximity of its receptors (2). Given that db/db mice are obese, circulating ATX levels may be extremely high. Our finding raises the possibility that, combined with high substrate levels, increased ATX could lead to increased local production of LPA, contributing to the endothelial dysfunction seen in diabetes. To clarify this, further experiments are needed.

As a part of the research plan did not result in publishable data, we started additional projects related to either new targets in endothelial dysfunction or to lysophospholipid biology.

1.2 Enhancement of sphingomyelinase-induced endothelial nitric oxide synthase-mediated vasorelaxation in a murine model of type 2 diabetes

Sphingolipids, derived from sphingomyelin metabolism, have been implicated as important mediators in the physiology and pathophysiology of the cardiovascular system (7-12). Sphingomyelinase (SMase) catalyzes the conversion of sphingomyelin to phosphoryl choline and ceramide, the latter is the precursor of other sphingolipid mediators, including ceramide-1-phosphate (C1P), sphingosine (Sph), and sphingosine-1-phosphate (S1P) (13). Normally, sphingomyelin (SM) represents about 10-20% of the lipids in the plasma membrane, mostly residing in the outer leaflet. However, most of these are found in the caveolae, and SMase is thought to be a regulator of lipid microdomains (14, 15). In the vasculature, SMases are implicated in the regulation of vascular tone and permeability as well as in causing atherosclerotic lesions and vascular wall remodeling (16). SMase enzymes are reportedly upregulated in certain cardiovascular and metabolic disorders such as T2DM (16-18). Although neutral Smase (nSMase) has been reported to induce a wide range of changes in the vascular tone, depending on the species, vessel type, and experimental conditions, relatively little is known about the effects of sphingolipids on vascular functions in T2DM. Therefore, we analyzed the effects of SMase on vascular tone under diabetic conditions in order to elucidate the signaling mechanisms involved.

First, we verified the general metabolic and vascular phenotype of T2DM mice tested in the study. The body weight increased almost 2-fold, whereas blood glucose levels increased 3-fold in db/db mice as compared to non-diabetic control littermates. Furthermore, the serum

phosphoryl choline level was also significantly increased in the diabetic group, which is consistent with the reported enhancement of SMase activity in type 2 diabetes (16-18). Vessels of db/db animals showed marked endothelial dysfunction indicated by the impairment of the dose-response relationship of acetylcholine (ACh)-induced vasorelaxation. These results confirm the T2DM-like metabolic and vascular phenotypes in db/db mice and suggest the *in vivo* enhancement of SMase activity as well.

Next, we determined the effect of nSMase on the active tone of control and db/db vessels. After phenylephrine (PE)-induced precontraction, 0.2 U/mL nSMase elicited additional contraction in control vessels that reached its maximum at 7.2 min before relaxing back to the pre-SMase level by the end of the 20-min observation period. In contrast, nSMase in db/db vessels elicited completely different responses. Surprisingly, after a marked initial relaxation during the first 5 min, the tone of the db/db vessels remained in a relaxed state below the level of the initial tension. Our next aim was to differentiate the constrictor and relaxant components of the vascular tension changes in response to nSMase. According to literature data (19-21), prostanoids acting on TP receptors have been implicated in mediating the vasoconstrictor effect of SMase. Therefore, we hypothesized that thromboxane prostanoid (TP) receptors also mediate the nSMase-induced vasoconstriction in our murine aorta model. Blockade of TP receptors not only abolished the vasoconstriction, but also converted it to a transient vasorelaxation in control vessels. This relaxation was even more strongly enhanced and prolonged in the db/db group. This finding was very surprising in light of the diminished ACh-induced vasorelaxation that we had observed in db/db animals, and was not consistent with the large body of literary data indicating diminished endothelium-dependent vasorelaxation in T2DM. Finally, we aimed to analyze the mechanism of the enhanced nSMase-induced vasorelaxation in vessels of db/db mice, whether it is due to the enhancement of eNOS-mediated vasorelaxation or to the onset of an NO-independent mechanism. After coadministration of eNOS inhibitor and TP receptor blockers, we could not detect considerable change in vascular tension neither in control, nor in db/db aortas upon nSMase treatment. Taken together, administration of nSMase induces TP receptor-mediated vasoconstriction and eNOS-mediated vasorelaxation in murine vessels. In spite of endothelial dysfunction in db/db mice, the vasorelaxant effect of nSMase is markedly augmented. A possible mechanism responsible for enhanced NO generation in T2DM can be the SMase-mediated disruption of sphingomyelin in endothelial lipid rafts, as this could interfere with the caveolar structure and induce the detachment of eNOS from caveolin-1, leading to high

amounts of NO released from the endothelium of db/db vascular rings. An intriguing interpretation of our finding is that retraction of eNOS in sphingomyelin-rich microdomains of the endothelial plasma membrane could contribute significantly to the development of vascular dysfunction in T2DM. We have prepared and submitted a manuscript containing these results which is currently under peer review and can be found attached to this report.

1.3 Characterization of Native and Human Serum Albumin-Bound Lysophosphatidic Acid Species and Their Effect on the Viability of Mesenchymal Stem Cells In Vitro

LPA, the product of ATX, also influences skeletal homeostasis and bone biology. In LPA_1 knock-out (KO) mice, decreased bone density, shorter bone length, and craniofacial dysmorphism can be observed. In contrast, LPA_4 KO mice show higher bone mass and trabecular number and thickness (22). Bone cells, such as marrow-derived mesenchymal stem cells (BM-dMSCs), osteoblasts, osteocytes, and osteoclasts play significant roles in bone homeostasis and repair. Under physiological conditions, osteoblast-produced LPA is present in bone tissue, and under some pathophysiological conditions, such as fracture healing, bone cells are exposed to high levels of platelet-derived LPA (23). In different bone cells, LPA induces various cellular effects, including proliferation, differentiation, survival, and migration (24).

Although, there is no direct evidence that BM-dMSCs produce LPA, autotaxin is secreted by human bone marrow-derived mesenchymal stem cells (hBM-dMSCs) (25). LPA receptors have been identified in different BM-dMSCs, however, in hBM-dMSCs LPA_1 was observed to be the most frequently detected LPA receptor (26). Different effects of LPA have been described in MSC biology. In addition to inducing migration (27), it was shown that LPA induces osteoblastic differentiation in hBM-dMSCs, which effect was completely absent in the case of LPA_1 inhibition, while the downregulation of LPA_4 expression increased osteogenesis (28). Furthermore, Chen *et al.* proved that LPA protects hBM-dMSCs against hypoxia and serum-deprivation-induced apoptosis (29). In another study, LPA was found to rescue BM-dMSCs from hydrogen peroxide-induced apoptosis (30). These findings suggest that LPA can act as a potent survival factor for MSCs.

In this project, we aimed to assess the complex formation between human serum albumin (HSA) and lysophosphatidic acid (LPA) in aqueous solutions and to determine the

effect of the most abundant, albumin-bound 16:0, 18:1, and 18:2 LPA species on the proliferation and migration of hBM-dMSCs.

To evaluate if the complex formation occurs between LPA and HSA, we investigated structure-related chemical changes with the use of Fourier-transform infrared (FTIR) spectroscopy. This method can be used to detect complex formation between LPA and HSA. The IR spectra were assessed for the three, physiologically most abundant 16:0, 18:1, and 18:2 LPA derivatives. According to our results, the spectral changes might indicate the binding of LPA species to HSA. Next, we performed XTT measurements to investigate the possible cytotoxicity and to determine the effects of 18:1, 18:2, and 16:0 LPA on the proliferation of hBM-dMSCs. 18:1 LPA in 1, 3, and 10 μM concentrations significantly increased cell proliferation compared to the control group, but solely when administered in the presence of HSA. In addition, 18:2 LPA significantly enhanced the proliferation of hBM-dMSCs in combination with HSA in 1, 3, and 10 μM and when examined alone in 3 and 10 μM concentrations. A significant elevation in the cell proliferation was caused by 0.3, 1, 3, and 10 μM 16:0 LPA treatment, exclusively in combination with HSA. To investigate if 18:1, 18:2, or 16:0 LPA influence the migration of the hBM-dMSCs, wound healing assay experiments were performed. Cell migration analysis showed no significant enhancement after LPA treatment, with or without HSA. Thus, it can be said that the observed cell proliferative effect of LPA treatment is not directly in connection with the enhanced migration of hBM-dMSCs. We published these results in 2022 in the Journal 'Applied Sciences'.

1.4 Acyl-chain specific effects of naturally occurring lysophosphatidic acids on vascular tone

LPA, the product of the ATX enzyme, has diverse roles in the vascular system, including the regulation of angiogenesis, remodeling, atherothrombosis and blood pressure. We reported recently that using isolated mouse aorta segments, LPA_1 receptor activation by the LPA1/3 agonist VPC31143 in the endothelium induces NO mediated relaxation, whereas in the vascular smooth muscle it evokes cyclooxygenase1 (COX1)-mediated thromboxane A_2 (TXA_2) release and vasoconstriction (31, 32). However, when the naturally occurring mono-unsaturated 18:1 LPA was tested (which is also the LPA form generally used in publications),

it had a full potency to evoke relaxation but had only minor constrictor activity. This puzzling result gave us the idea to test more, naturally occurring LPA species on the vascular tone.

In the plasma, the concentration of LPA is about 100 nM and the most common forms are 18:2>18:1>18:0>16:0>20:4. Its concentration is elevated up to 10 μM in the serum due to platelet activation, and also the proportion of the LPA isoforms is changed to 20:4>18:2>16:0>18:1>18:0 (33). Interestingly, the amount of LPA is also elevated in the plasma of patients with acute coronary syndrome (34), especially the level of the 18:2 and 20:4 LPAs (35). To date, very little is known about the direct effect of the naturally occurring LPA species on the vascular tone. Therefore, the main objective of this study was to determine the activity of eight commercially available, naturally occurring LPA species in endothelium-intact and endothelium-denuded mouse aorta.

First, we assessed the effect of the different LPA species in PE precontracted, endothelium-intact thoracic aorta segments with wire myography. We investigated the 14:0, 16:0, 18:0 and 20:0 saturated LPAs. Representative recordings show that only the 14:0 and 16:0 LPAs were able to elicit vasorelaxation (Fig.1.A). The disappearance of the relaxant effect is associated with the length of fatty acid chain: the longer the fatty acid chain the slighter the relaxation. In the case of the 14:0 and 16:0 LPAs, we tested their relaxant effect on vessels prepared from LPA_1-KO animals. As shown in Figure 1B, the relaxant effect diminished in the vessels prepared from LPA_1-KO mice, suggesting that the elicited vasorelaxation is triggered by the LPA_1 receptor. 18:0 and 20:0 LPAs did not elicit vasorelaxation (Fig.1C).

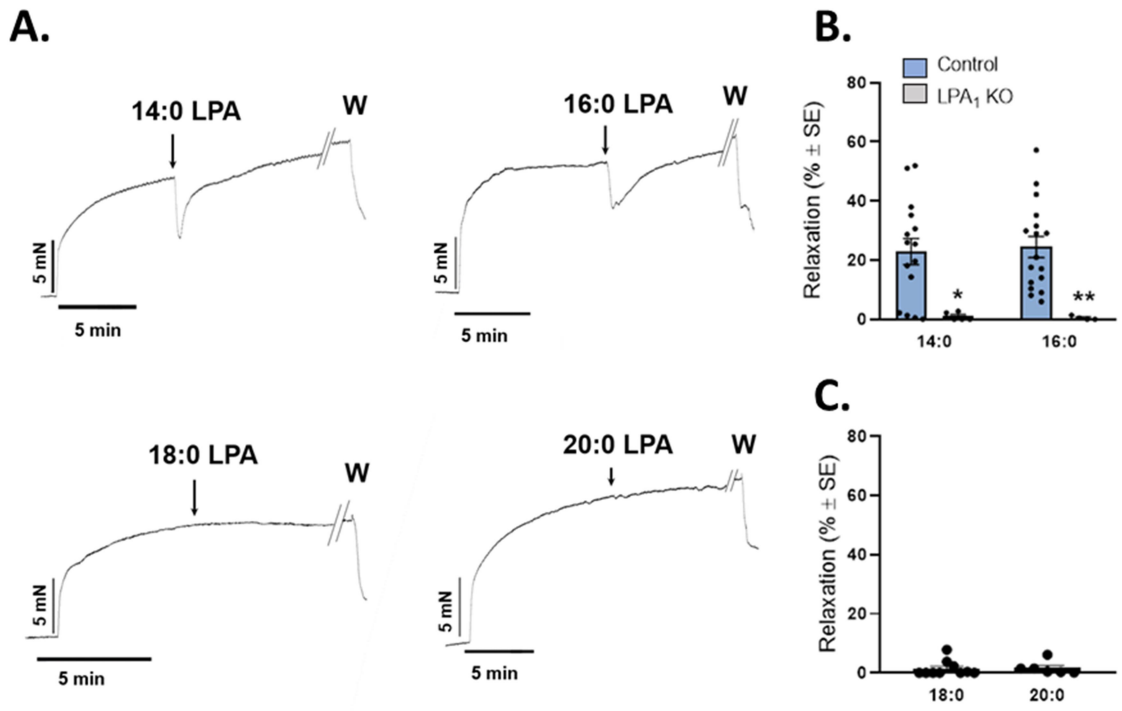

Figure 1. Representative recordings of vasorelaxation induced by saturated LPA in PE precontracted vessels. Arrows indicate the administration of 10 μM LPA, W stands for washing out (**A**). Vasorelaxation induced by 14:0 and 16:0 LPA (10 μM of each) in vessels from WT (Control) and LPA_1 KO mice [n=15, 17 (Control) and 6, 5 (LPA_1 KO); one-way ANOVA followed by Tukey's multiple comparisons test] (**B**). Vasorelaxation induced by 18:0 and 20:0 LPA in WT mice (10 μM of each LPA; n= 10, 6; unpaired Student's t-test) (**C**). *p<0.05, **p<0.01. Bars represent mean±SEM

In the next step, vasorelaxant activity of 18:1, 18:2, 18:3 and 20:4 LPA (10 μM of each) was tested. Representative recordings of the vasorelaxation induced by unsaturated LPAs illustrate that 18:1 LPA elicited a marked vasorelaxation, however in the case of polyunsaturated LPAs the relaxation decreases and becomes more transient (Fig.2A). To identify the receptor responsible for the vasorelaxation, we tested the effect of the unsaturated LPAs in aortic segments isolated from LPA_1-KO mice. Surprisingly in the case of poly-unsaturated LPAs after the relaxation the vascular tone did not stabilizes at the level of the precontraction, as seen in the case of 18:1 LPA, but an additional contraction appears. Unsaturated LPAs failed to induce vasorelaxation in vessels prepared from LPA_1-KO animals, suggesting that these LPAs elicit vasorelaxation via LPA_1 receptor as well (Fig.2.B). As the 20:4 LPA has only a slight relaxant effect, only 18C LPAs were used for further analysis. We have previously reported that LPA_1 receptor activation can evoke both vasorelaxation and vasoconstriction (31, 32). We hypothesized that in the case of endothelium

intact aortic segments, we see the superimposition of these two opposite effects on the vascular tone. To examine the relaxant activity alone, the LPA induced constrictor response had to be inhibited, therefore we applied the 18C LPAs to vessels treated with 10 μM indomethacin. When comparing the maximal elicited vasorelaxation induced by these LPAs, only the 18:3 LPA induced vasorelaxation was significantly increased in the COX inhibited aortic segments (Fig.2C). However, analyzing the area over curve of the 18C LPA induced vasorelaxation within 5 minutes after administering the LPAs, vasorelaxation induced by both polyunsaturated LPA species was notably increased in the presence of indomethacin (Fig.2D). No significant difference was detected in the relaxant activity of the investigated C18 LPAs in vessels treated with indomethacin, indicating that the cause of the acyl chain dependent differences in vasoactivity may be related to alterations in their constrictor capacity.

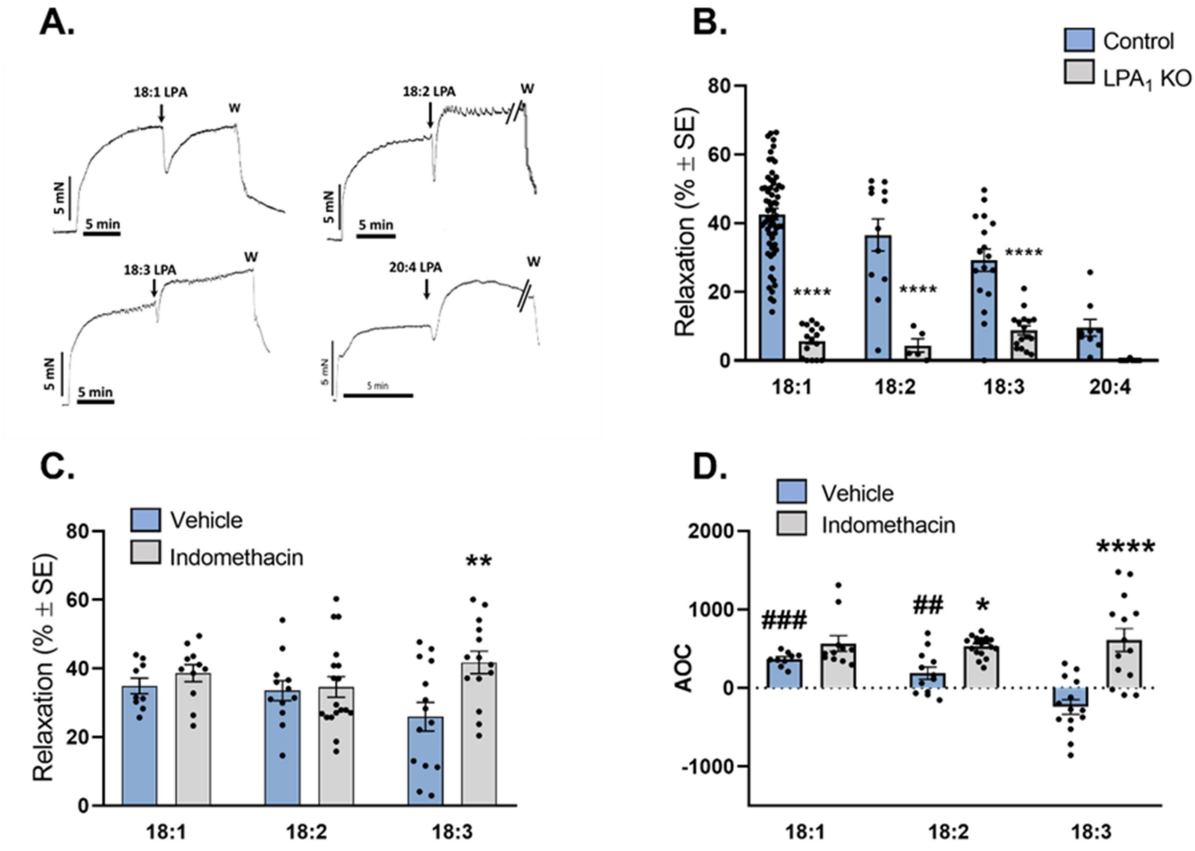

Figure 2 Representative recordings of vasorelaxation elicited by 10 μM unsaturated LPAs in PE precontracted vessels. Arrows indicate the administration of LPA, W stands for washing out **(A)**. Vasorelaxant activity of unsaturated LPAs (10 μM of 18:1, 18:2, 18:3, and 20:4 LPAs) in vessels from WT (Control) and LPA_1 KO mice [n=62, 12, 17, 9 (Control) and 17, 5, 16, 9 (LPA_1 KO); two-way ANOVA followed by Sidak's multiple comparisons test; ****p<0.0001 vs. Control] **(B)**. Relaxation induced by 18C LPAs (10 μM of 18:1, 18:2, and 18:3 LPA) in vessels treated with vehicle or indomethacin [n=9, 12, 14 (Control) 11, 18, 14

(Indomethacin); two-way ANOVA followed by Sidak's multiple comparisons test; **p<0.01 vs. Vehicle] **(C)**. Area over curve (AOC) of vasorelaxation induced by 18C LPAs (10 µM of each) in vessels treated with vehicle or indomethacin. [n=9, 12, 14 (Control) 11, 18, 14 (Indomethacin); two-way ANOVA followed by Sidak's multiple comparisons test; *p<0.05 vs. Vehicle, ****p<0.0001 vs. Vehicle; ###p<0.001 vs. 18:3 Vehicle, ##p<0.01 vs. 18:3 Vehicle] **(D)**. Bars represent mean±SEM.

As in our previous study vasoconstriction induced by LPA_1 receptor activation was significantly higher in AA segments compared to TA segments (31), LPA species were applied on the resting tone of endothelium-denuded AA segments. Among the saturated LPAs (10 µM of 14:0, 16:0, 18:0 and 20:0 LPA) only the 14:0 LPA has constrictor property (Fig.3.A). As shown on representative recordings (Fig.3B), vasoconstriction induced by unsaturated LPAs (10 µM of 18:1, 18:2, 18:3 and 20:4 LPA) has an increasing trend in parallel with the level of unsaturation. Dose-response curve fitting showed both increased efficacy and potency of the constrictor activity of poly-unsaturated LPA species (18:2, 18:3, and 20:4 LPA) (Fig.3C, D).

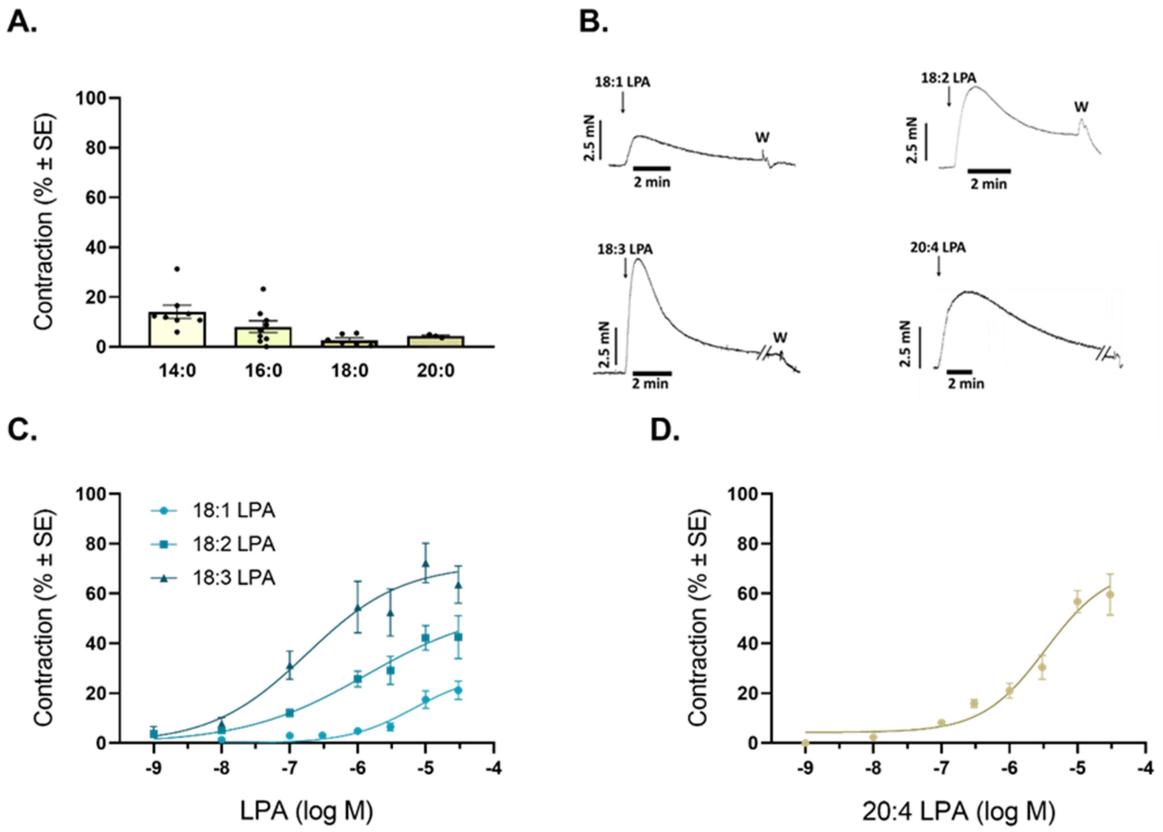

Figure 3 Constrictor activity of saturated LPA species (10 µM of 14:0, 16:0, 18:0, and 20:0; n=10, 9, 6, 3; one-way ANOVA; bars represent mean±SEM) (**A**). Representative recordings of vasoconstriction induced by 10 µM unsaturated LPAs in aortic vessel rings from WT mice. Arrows indicate the administration of 10 µM LPA, W stands for washing out (**B**). Dose-

response curve fittings for 18:1 (EC_{50}:6.67, E_{max}:27.9%), 18:2 (EC_{50}:1.35 μM, E_{max}:57.8%), and 18:3 LPA (EC_{50}:0.18 μM, E_{max}:71.6%) induced vasoconstriction in vessels from WT mice (**C**). Dose response curve fitting for 20:4 LPA (EC_{50}:3.3 μM, E_{max}:70.7 %) induced vasoconstriction in vessels from WT mice (**D**).

Next, we examined the constrictor effect of those LPA species, which have considerable constrictor activity, in AA segment isolated from LPA_1-KO mice (Fig.4A). Vasoconstriction induced by 14:0 and 18C LPAs was completely abolished in the vessels prepared from LPA_1-KO mice. In contrast, in the aortic segments of LPA_1-KO mice, a significant proportion of vasoconstriction elicited by 20:4 LPA was preserved, indicating that another signaling pathway is involved in its constrictor effect. To gain better understanding of the structure-activity relationship of vasoconstriction, for further analyses we only investigated unsaturated 18C LPA species, as they evoke remarkable constriction, entirely mediated by LPA_1 receptor. Inhibiting COX with indomethacin, vasoconstriction evoked by unsaturated 18C LPA completely disappeared (Fig.4B). As COX activation leads to the release of the potent vasoconstrictor, thromboxane, we aimed to measure the released TXB_2, which is a stable metabolite of TXA_2, in the supernatants of vessels exposed to 10 μM of each 18C LPA. Polyunsaturated 18:2 and 18:3 LPAs increased the TXB_2 production of the aortic segments, but not 18:1 LPA, suggesting the role of prostanoids in the increased constrictor effect. As COX activation is closely linked to the Gi protein signaling pathway, we investigated the participation of the Gi protein in the constrictor activity of the 18C LPAs. Mice were treated with PTX intraperitoneally for 5 days. Average contraction induced by 18:2 and 18:3 LPA was significantly decreased in the vessels isolated from mice treated with PTX compared to the aortic segments of mice treated with vehicle (Fig.4D).

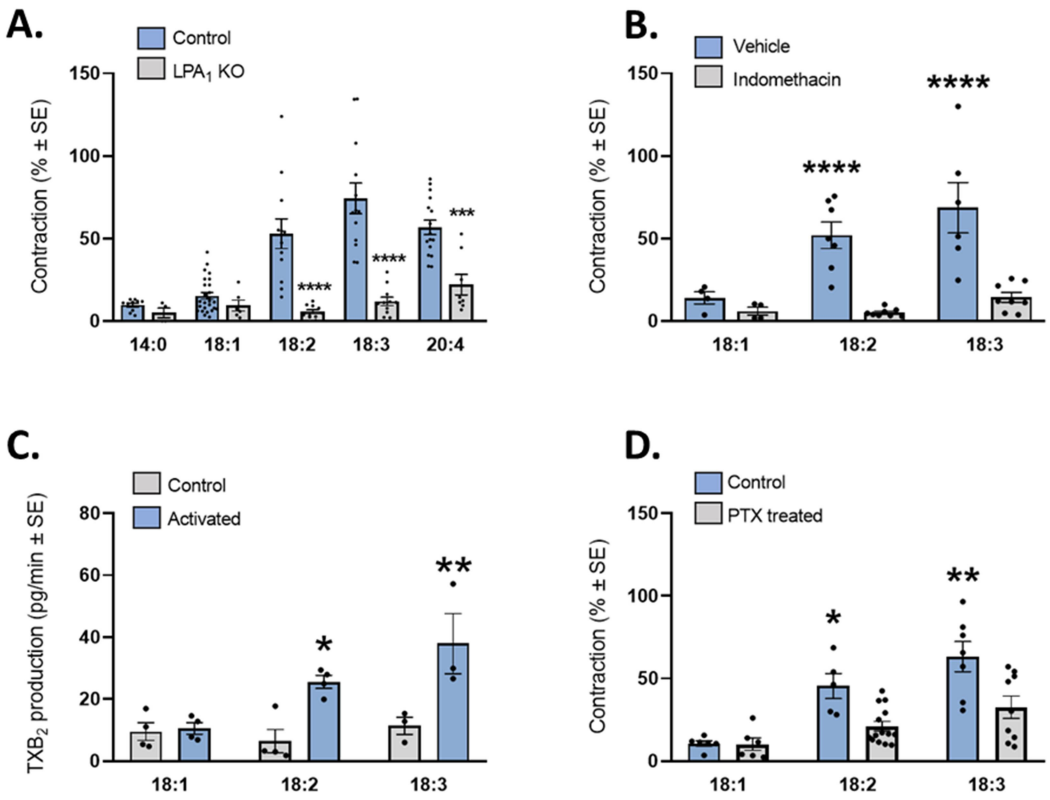

Figure 4 The 14:0, 18:1, 18:2, 18:3, and 20:4 LPA (10 μM) elicited vasoconstriction in vessels from WT (Control) and LPA_1 KO mice [n=10, 27, 12, 13, 16 (Control) and 4, 6, 10, 11, 8 (LPA_1 KO); two-way ANOVA, followed by Sidak's multiple comparisons test] (**A**). The 18C LPA (10 μM of each) induced vasoconstriction in WT (Control) and COX inhibited (Indomethacin) vessels [n=4, 7, 6 (Control) and 4, 8, 8 (Indomethacin); two-way ANOVA, followed by Sidak's multiple comparisons test] (**B**). TXB_2 production in vessels before (Control) and after (Activated) treated with 10 μM of 18C LPA [n=4, 4, 3 (Control) and 4, 4, 3 (Activated); two-way ANOVA, followed by Sidak's multiple comparisons test] (**C**). Vasoconstriction elicited by 18C LPA (10 μM of 18:1, 18:2, 18:3 LPA) in vessels from mice treated with vehicle (Control) or pertussis toxin (PTX treated) [n=6, 5, 7 (Control) and 6, 14, 9 (PTX treated); two-way ANOVA, followed by Sidak's multiple comparisons test] (**D**). *p<0.05; **p<0.01; ****p<0.0001. Bars represent mean ± SEM.

To get a better insight of the molecular mechanism underlying both the relaxant and constrictor activity, next we measured the intracellular Ca^{2+} signal after the administration of each 18C LPA in primary endothelial and vascular smooth muscle cell cultures (VSMC). Endothelial cells showed a marked intracellular Ca^{2+}-increase when stimulated by 10 μM of 18C LPA (Fig.5A, B). In contrast to the endothelial cells, VSMCs exhibited negligible Ca^{2+} signal upon administration of 18C LPA (10 μM of each), suggesting that there are cell specific differences in the signaling of these LPAs (Fig.5C, D), and raises further questions

about the exact signaling mechanism underlying LPA_1-mediated thromboxane release and vasoconstriction.

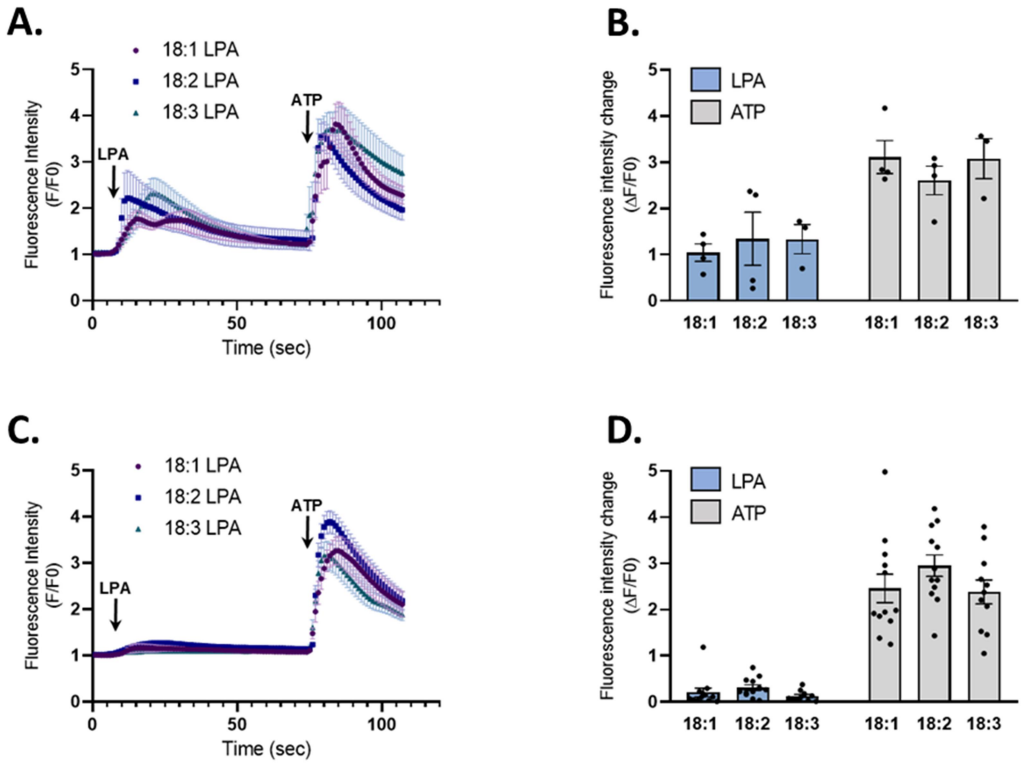

Figure 5 Average trace of fluorescent intensity in Fluo-4AM loaded endothelial cells isolated from the aorta of WT mice. Administration of 10 µM of 18C LPAs, and 10 µM of ATP are indicated by arrows (n=4, 4, 3) (**A**). Increase in fluorescent intensity evoked by 18C LPA or ATP (10 µM of each) [n=4, 4, 3 (LPA); 4, 4, 3 (ATP); two-way ANOVA followed by Sidak's multiple comparisons test] (**B**). Average trace of fluorescent intensity in Fluo-4 AM loaded VSMCs isolated from the aorta of WT mice. Administration of LPA, and ATP (10 µM of each) are indicated by arrows (n= 12, 12, 11) (**C**). 18C LPA (10 µM) evoked maximal fluorescent intensity change in percentage of the 10 µM ATP elicited maximal fluorescent signal [n=12, 12, 11; two-way ANOVA followed by Sidak's multiple comparisons test] (**D**). *p<0.05; **p<0.01; ****p<0.0001. Bars represent mean ± SEM.

Taken together, different naturally occurring LPA species have very different vasoactive effects. However, all these effects are mediated by the activation of LPA_1 receptor, there might be cell specific differences in the signaling pathways. Shorter chain, saturated LPAs have a weak relaxing, and negligible constrictor effect, but as the chain becomes longer, these effects disappear. On the other hand, unsaturated LPAs have higher potency to evoke both the vasorelaxation and the vasoconstriction. This is in accordance with the literature data, as polyunsaturated LPA species might be stronger agonists of the LPA_1 receptor (36). Regarding the endothelial effects of the investigated polyunsaturated LPAs, their vasorelaxant

activity decreases with the degree of unsaturation, but this seems not to be due to their ability to induce NO, but rather due to a counteracting vasoconstrictor activity appearing only when polyunsaturated LPAs were tested. This is also supported by the Ca^{2+} measurement data in endothelial cells. We found that only polyunsaturated LPA species can evoke thromboxane production in the thoracic aorta, but interestingly, this effect is not due to increased intracellular Ca^{2+} release by these LPA species in the smooth muscle cells. In conclusion, polyunsaturated LPA species have strong vasoconstrictor activity, due to their ability to increase COX mediated thromboxane release. This constriction is present even in endothelium intact aortic segments, where it counteracts LPA-mediated vasorelaxation, but is particularly interesting in case of endothelial injury and platelet activation where polyunsaturated LPAs can contribute to the progression of vasospasm via initiating thromboxane-mediated signaling. We are currently preparing a manuscript with these results and plan to submit it for publication by summer, 2023.

1.5 Signal transduction pathways of unsaturated lysophosphatidic acid species evoked vasoconstriction

Based on the study described in detail in the previous section, we further analyzed the signaling mechanism of the LPA induced vasoconstriction. For the experiments, 18:2 LPA was chosen, as it is one of the most abundant form of LPA under both physiological and pathophysiological conditions. As in the previous study, we did not see considerable intracellular Ca^{2+} increase upon LPA treatment in isolated VSMC, we started to do measurements with confocal wire myography. This technique is suitable to visualize the Ca^{2+}-changes and vascular tone simultaneously in isolated vessels. First, we removed both the endothelium and adventitia, and loaded the remaining smooth muscle layer with Fura-2AM. Surprisingly, removal of the adventitia abolished the 18:2 LPA induced vasoconstriction and the elicited Ca^{2+}-response was minimal. On the other hand, phenylephrine- and potassium-induced contraction and Ca^{2+} signals were clearly visible, indicating the integrity of the smooth muscle layer and its ability to constrict upon stimulation. Interestingly, when only the adventitia was pulled on the pins of the confocal myograph, a marked Ca^{2+}-signal was detectable upon 18:2 LPA administration.

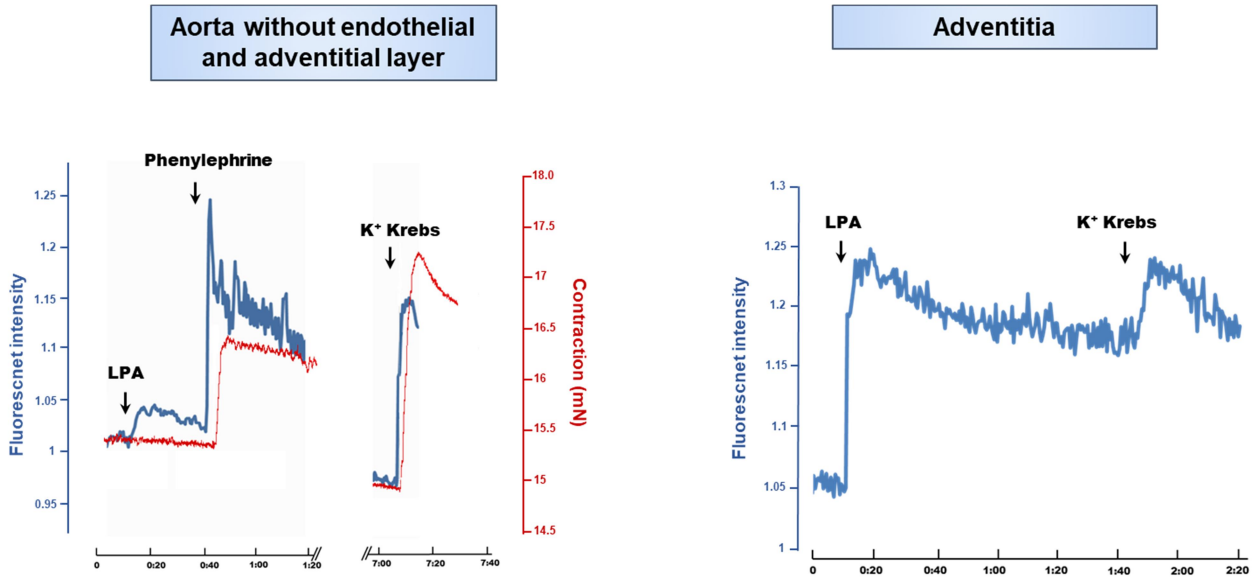

This difference was also present, when isolated vascular smooth muscle cells were compared to isolated adventitial cells. In a primary isolated vascular smooth muscle cell culture, 18:2 LPA elicited only minimal changes in the intracellular Ca^{2+}. The purity of the culture was verified by α-SMA (smooth muscle actin) staining. A mixed culture of isolated adventitial cells was thereafter tested. In some of the cells, there was a prominent Ca^{2+}-signal. After the cells were fixed and stained, we concluded that only those cells showed the Ca^{2+}-signal, which were positive for LPA_1 receptor but negative for the smooth muscle marker.

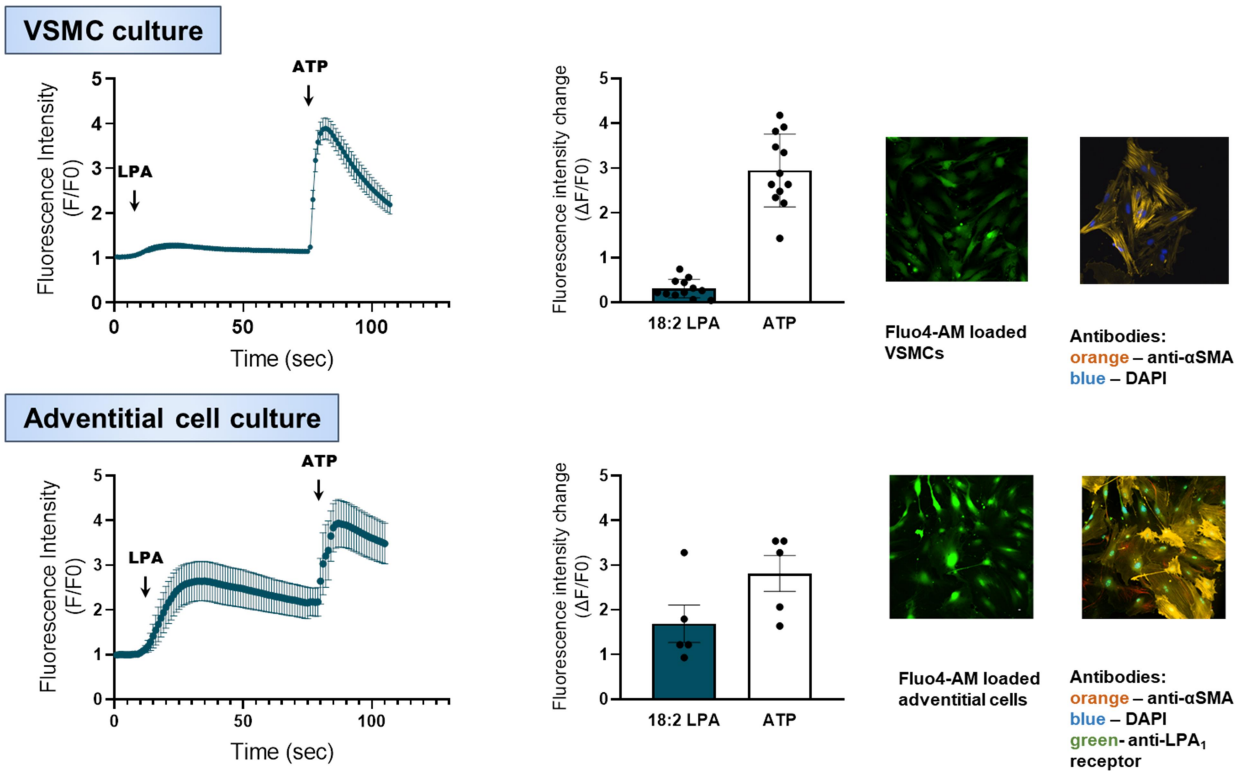

We wanted to further analyze the localization of LPA_1 receptor in the mouse aorta. First, we demonstrated that the antibody of our choice is indeed specific for LPA_1 receptor. On the left side of the following figure, red fluorescence shows the presence of the LPA_1 receptor in the aortic section, which is completely missing in the aorta prepared from Lpar1 KO mouse. *En face* staining of the aorta showed that the tunica adventitia expresses the LPA_1 receptor, while the tunica media does not (right side of the next figure). This finding is opposed to our previous publication where we described LPA_1 receptor expression on primary isolated aortic VSMC with qPCR (31), but also highlights the limitations of qPCR technique, as detectable mRNA of a membrane receptor does not necessarily mean that sufficient amount of the receptor is present in the membrane (to be detected by immunostaining or more importantly, to induce any biological effects).

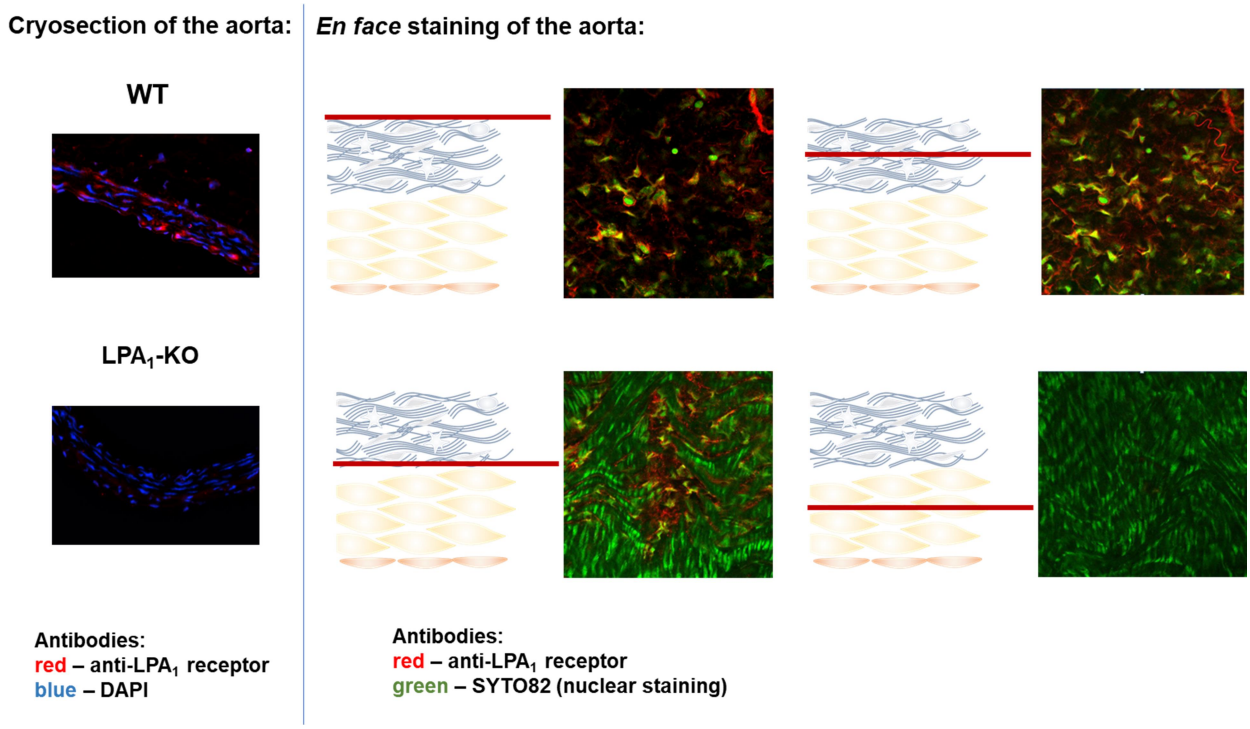

We also confirmed the importance of the tunica adventitia in the vasoconstrictor effect of 18:2 LPA, as well as its role in the thromboxane production upon 18:2 LPA treatment. In accordance to this, we were able to detect significantly higher Lpar1 expression with qPCR when the adventitia was not removed from the aorta. Further experiments are planned to find out, which cell population of the adventitia is responsible for the vasoconstrictor effects of 18:2 LPA. We plan to prepare a manuscript with these results and submit it for publication by the end of 2023.

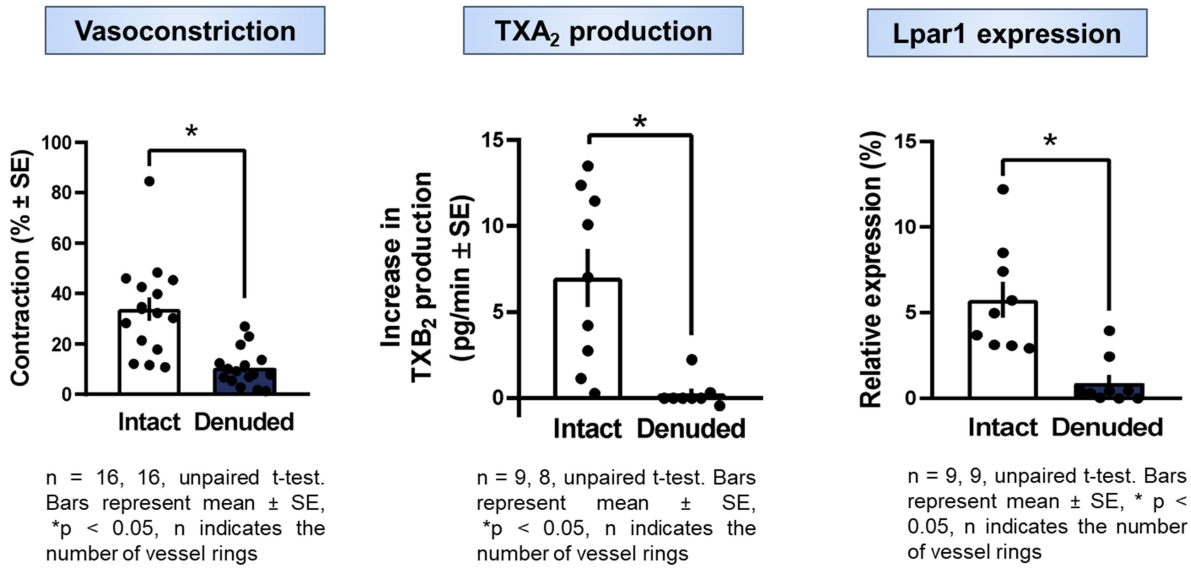

n = 16, 16, unpaired t-test. Bars represent mean ± SE, *p < 0.05, n indicates the number of vessel rings

n = 9, 8, unpaired t-test. Bars represent mean ± SE, *p < 0.05, n indicates the number of vessel rings

n = 9, 9, unpaired t-test. Bars represent mean ± SE, * p < 0.05, n indicates the number of vessel rings

1. Vanhoutte, P. M., Shimokawa, H., Tang, E. H., Feletou, M. (2009) Endothelial dysfunction and vascular disease. Acta Physiol (Oxf) 196: 193-222

2. Moolenaar, W. H., Perrakis, A. (2011) Insights into autotaxin: how to produce and present a lipid mediator. Nat Rev Mol Cell Biol 12: 674-679

3. Yung, Y. C., Stoddard, N. C., Chun, J. (2014) LPA receptor signaling: pharmacology, physiology, and pathophysiology. J Lipid Res 55: 1192-1214

4. Miyabe, C., Miyabe, Y., Nagai, J., Miura, N. N., Ohno, N., et al. (2019) Abrogation of lysophosphatidic acid receptor 1 ameliorates murine vasculitis. Arthritis Research & Therapy 21: 191

5. Lam, T. Y., Seto, S. W., Lau, Y. M., Au, L. S., Kwan, Y. W., et al. (2006) Impairment of the vascular relaxation and differential expression of caveolin-1 of the aorta of diabetic +db/+db mice. Eur J Pharmacol 546: 134-141

6. Dusaulcy, R., Rancoule, C., Grès, S., Wanecq, E., Colom, A., et al. (2011) Adipose-specific disruption of autotaxin enhances nutritional fattening and reduces plasma lysophosphatidic acid. Journal of Lipid Research 52: 1247-1255

7. Peters, S. L., Alewijnse, A. E. (2007) Sphingosine-1-phosphate signaling in the cardiovascular system. Curr Opin Pharmacol 7: 186-192

8. Igarashi, J., Michel, T. (2009) Sphingosine-1-phosphate and modulation of vascular tone. Cardiovasc Res 82: 212-220

9. Kerage, D., Brindley, D. N., Hemmings, D. G. (2014) Review: novel insights into the regulation of vascular tone by sphingosine 1-phosphate. Placenta 35 Suppl: S86-92

10. Proia, R. L., Hla, T. (2015) Emerging biology of sphingosine-1-phosphate: its role in pathogenesis and therapy. J Clin Invest 125: 1379-1387

11. Hemmings, D. G. (2006) Signal transduction underlying the vascular effects of sphingosine 1-phosphate and sphingosylphosphorylcholine. Naunyn Schmiedebergs Arch Pharmacol 373: 18-29

12. De Palma, C., Meacci, E., Perrotta, C., Bruni, P., Clementi, E. (2006) Endothelial nitric oxide synthase activation by tumor necrosis factor alpha through neutral sphingomyelinase 2, sphingosine kinase 1, and sphingosine 1 phosphate receptors: a novel pathway relevant to the pathophysiology of endothelium. Arterioscler Thromb Vasc Biol 26: 99-105

13. Fyrst, H., Saba, J. D. (2010) An update on sphingosine-1-phosphate and other sphingolipid mediators. Nat Chem Biol 6: 489-497

14. Mitsutake, S., Zama, K., Yokota, H., Yoshida, T., Tanaka, M., et al. (2011) Dynamic modification of sphingomyelin in lipid microdomains controls development of obesity, fatty liver, and type 2 diabetes. J Biol Chem 286: 28544-28555

15. Romiti, E., Meacci, E., Tanzi, G., Becciolini, L., Mitsutake, S., et al. (2001) Localization of neutral ceramidase in caveolin-enriched light membranes of murine endothelial cells. FEBS Lett 506: 163-168

16. Pavoine, C., Pecker, F. (2009) Sphingomyelinases: their regulation and roles in cardiovascular pathophysiology. Cardiovasc Res 82: 175-183

17. Shamseddine, A. A., Airola, M. V., Hannun, Y. A. (2015) Roles and regulation of neutral sphingomyelinase-2 in cellular and pathological processes. Adv Biol Regul 57: 24-41

18. Russo, S. B., Ross, J. S., Cowart, L. A. (2013) Sphingolipids in obesity, type 2 diabetes, and metabolic disease. Handb Exp Pharmacol: 373-401

19. Spijkers, L. J., van den Akker, R. F., Janssen, B. J., Debets, J. J., De Mey, J. G., et al. (2011) Hypertension is associated with marked alterations in sphingolipid biology: a potential role for ceramide. PLoS One 6: e21817

20. van den Elsen, L. W., Spijkers, L. J., van den Akker, R. F., van Winssen, A. M., Balvers, M., et al. (2014) Dietary fish oil improves endothelial function and lowers blood pressure via suppression of sphingolipid-mediated contractions in spontaneously hypertensive rats. Journal of hypertension 32: 1050-1058; discussion 1058

21. Spijkers, L. J., Janssen, B. J., Nelissen, J., Meens, M. J., Wijesinghe, D., et al. (2011) Antihypertensive treatment differentially affects vascular sphingolipid biology in spontaneously hypertensive rats. PLoS One 6: e29222

22. Salles, J. P., Laurencin-Dalicieux, S., Conte-Auriol, F., Briand-Mesange, F., Gennero, I. (2013) Bone defects in LPA receptor genetically modified mice. Biochim Biophys Acta 1831: 93-98

23. Karagiosis, S. A., Karin, N. J. (2007) Lysophosphatidic acid induces osteocyte dendrite outgrowth. Biochem Biophys Res Commun 357: 194-199

24. Yu, Z. L., Jiao, B. F., Li, Z. B. (2018) Lysophosphatidic Acid Analogue rather than Lysophosphatidic Acid Promoted the Bone Formation In Vivo. Biomed Res Int 2018: 7537630

25. Kanehira, M., Fujiwara, T., Nakajima, S., Okitsu, Y., Onishi, Y., et al. (2016) A Lysophosphatidic Acid Receptors 1 and 3 Axis Governs Cellular Senescence of Mesenchymal Stromal Cells and Promotes Growth and Vascularization of Multiple Myeloma. Stem Cells 35: 739-753

26. Wu, X., Ma, Y., Su, N., Shen, J., Zhang, H., et al. (2019) Lysophosphatidic acid: Its role in bone cell biology and potential for use in bone regeneration. Prostaglandins Other Lipid Mediat 143: 106335

27. Lee, M. J., Jeon, E. S., Lee, J. S., Cho, M., Suh, D. S., et al. (2008) Lysophosphatidic acid in malignant ascites stimulates migration of human mesenchymal stem cells. J Cell Biochem 104: 499-510

28. Liu, Y. B., Kharode, Y., Bodine, P. V., Yaworsky, P. J., Robinson, J. A., et al. (2010) LPA induces osteoblast differentiation through interplay of two receptors: LPA1 and LPA4. J Cell Biochem 109: 794-800

29. Chen, J., Baydoun, A. R., Xu, R., Deng, L., Liu, X., et al. (2008) Lysophosphatidic acid protects mesenchymal stem cells against hypoxia and serum deprivation-induced apoptosis. Stem Cells 26: 135-145

30. Wang, X.-Y., Fan, X.-S., Cai, L., Liu, S., Cong, X.-F., et al. (2015) Lysophosphatidic acid rescues bone mesenchymal stem cells from hydrogen peroxide-induced apoptosis. Apoptosis 20: 273-284

31. Dancs, P. T., Ruisanchez, E., Balogh, A., Panta, C. R., Miklos, Z., et al. (2017) LPA1 receptor-mediated thromboxane A2 release is responsible for lysophosphatidic acid-induced vascular smooth muscle contraction. FASEB J

32. Ruisanchez, É., Dancs, P., Kerék, M., Németh, T., Faragó, B., et al. (2014) Lysophosphatidic acid induces vasodilation mediated by LPA1 receptors, phospholipase C, and endothelial nitric oxide synthase. FASEB J 28: 880-890

33. Baker, D. L., Desiderio, D. M., Miller, D. D., Tolley, B., Tigyi, G. J. (2001) Direct quantitative analysis of lysophosphatidic acid molecular species by stable isotope dilution electrospray ionization liquid chromatography-mass spectrometry. Anal Biochem 292: 287-295

34. Dohi, T., Miyauchi, K., Ohkawa, R., Nakamura, K., Kishimoto, T., et al. (2012) Increased circulating plasma lysophosphatidic acid in patients with acute coronary syndrome. Clin Chim Acta 413: 207-212

35. Kurano, M., Kano, K., Dohi, T., Matsumoto, H., Igarashi, K., et al. (2017) Different origins of lysophospholipid mediators between coronary and peripheral arteries in acute coronary syndrome. J Lipid Res 58: 433-442

36. Fujiwara, Y., Sardar, V., Tokumura, A., Baker, D., Murakami-Murofushi, K., et al. (2005) Identification of residues responsible for ligand recognition and regioisomeric selectivity of lysophosphatidic acid receptors expressed in mammalian cells. Journal of Biological Chemistry 280: 35038-35050

Autotaxin-Lysophosphatidic Acid Receptor 5 Axis Evokes Endothelial Dysfunction *via* Reactive Oxygen Species Signaling

Journal:	*Experimental Biology and Medicine*
Manuscript ID	EBM-22-RM-1155
Manuscript Type:	Original Research
Date Submitted by the Author:	28-Dec-2022
Complete List of Authors:	Janovicz, Anna; Semmelweis University, Institute of Translational Medicine; Eötvös Loránd Research Network and Semmelweis University (ELKH-SE) Cerebrovascular and Neurocognitive Disorders Research Group Majer, Aliz; Semmelweis University, Institute of Translational Medicine Kosztelnik, Mónika ; Semmelweis University, Institute of Translational Medicine; Eötvös Loránd Research Network and Semmelweis University (ELKH-SE) Cerebrovascular and Neurocognitive Disorders Research Group Geiszt, Miklós; Semmelweis University, Department of Physiology Chun, Jerold; Sanford Burnham Prebys Medical Discovery Institute Ishii, Satoshi; Akita University Graduate School of Medicine School of Medicine, Department of Immunology Tigyi, Gabor; University of Tennessee Health Science Center, Department of Physiology; Semmelweis University, Institute of Translational Medicine Benyó, Zoltán; Semmelweis University, Institute of Translational Medicine; Eötvös Loránd Research Network and Semmelweis University (ELKH-SE) Cerebrovascular and Neurocognitive Disorders Research Group Ruisanchez, Éva; Semmelweis University, Institute of Translational Medicine; Eötvös Loránd Research Network and Semmelweis University (ELKH-SE) Cerebrovascular and Neurocognitive Disorders Research Group
Keywords:	lysophosphatidylcholine, autotaxin, lysophosphatidic acid, lysophosphatidic acid receptor 5, endothelial dysfunction, reactive oxygen species
Abstract:	Lysophosphatidylcholine (LPC) is a bioactive lipid that has been shown to attenuate endothelium-dependent vasorelaxation contributing to endothelial dysfunction, however, the underlying mechanisms are not well understood. In the present study we investigated the molecular mechanisms involved in the development of LPC-evoked impairment of endothelium-dependent vasorelaxation. In aortic rings isolated from wild-type (WT) mice, a 20 min exposure to LPC significantly reduced the acetylcholine (ACh)-induced vasorelaxation indicating the impairment of normal endothelial function. Interestingly, pharmacological inhibition of autotaxin (ATX) by GLPG1690 partially reversed the endothelial dysfunction, suggesting that lysophosphatidic acid (LPA) derived from LPC may be involved in the effect. Therefore, the effect of LPC was also tested in aortic rings isolated from different LPA receptor knock-out (KO) mice. LPC evoked a marked reduction in ACh-dependent vasorelaxation in *Lpar1*, *Lpar2*, and *Lpar4* KO, but its effect was significantly attenuated

	in *Lpar5* KO vessels. Furthermore, addition of superoxide dismutase reduced the LPC-induced endothelial dysfunction in WT but not in the *Lpar5* KO mice. In addition, LPC increased H_2O_2 release from WT vessels, which was significantly reduced in *Lpar5* KO vessels. Our findings indicate that the ATX-LPA-LPA_5 receptor axis is involved in the development of LPC-induced impairment of endothelium-dependent vasorelaxation *via* LPA_5 receptor mediated reactive oxygen species production. Taken together, in this study we identified a new pathway contributing to the development of LPC-induced endothelial dysfunction.

Title

Autotaxin-Lysophosphatidic Acid Receptor 5 Axis Evokes Endothelial Dysfunction *via* Reactive Oxygen Species Signaling

Running title

Lysophosphatidic Acid Signaling in Endothelial Dysfunction

Authors

Anna Janovicz[1,2], Aliz Majer[1], Mónika Kosztelnik[1,2], Miklós Geiszt[3], Jerold Chun[4], Satoshi Ishii[5], Gábor József Tigyi[1,6], Zoltán Benyó[1,2,] Éva Ruisanchez[1,2]

[1]Institute of Translational Medicine, Semmelweis University, Budapest H-1094, Hungary

[2]Eötvös Loránd Research Network and Semmelweis University (ELKH-SE) Cerebrovascular and Neurocognitive Disorders Research Group, Budapest H-1052, Hungary

[3]Faculty of Medicine, Department of Physiology, Semmelweis University H-1094, Budapest, Hungary

[4]Translational Neuroscience at Sanford Burnham Prebys Medical Discovery Institute, La Jolla CA 92037, USA

[5]Department of Immunology, Graduate School of Medicine, Akita University, Akita 010-8543, Japan

[6]Department of Physiology, University of Tennessee Health Science Center, Memphis TN 38163, USA

Corresponding Author

Éva Ruisanchez, Institute of Translational Medicine, Semmelweis University, 37-47 Tűzoltó Street, Budapest H-1094, Hungary. (e-mail: ruisanchez.eva@med.semmelweis-univ.hu)

Abstract

Lysophosphatidylcholine (LPC) is a bioactive lipid that has been shown to attenuate endothelium-dependent vasorelaxation contributing to endothelial dysfunction, however, the underlying mechanisms are not well understood. In the present study we investigated the molecular mechanisms involved in the development of LPC-evoked impairment of endothelium-dependent vasorelaxation. In aortic rings isolated from wild-type (WT) mice, a 20 min exposure to LPC significantly reduced the acetylcholine (ACh)-induced vasorelaxation indicating the impairment of normal endothelial function. Interestingly, pharmacological inhibition of autotaxin (ATX) by GLPG1690 partially reversed the endothelial dysfunction, suggesting that lysophosphatidic acid (LPA) derived from LPC may be involved in the effect. Therefore, the effect of LPC was also tested in aortic rings isolated from different LPA receptor knock-out (KO) mice. LPC evoked a marked reduction in ACh-dependent vasorelaxation in *Lpar1*, *Lpar2*, and *Lpar4* KO, but its effect was significantly attenuated in *Lpar5* KO vessels. Furthermore, addition of superoxide dismutase reduced the LPC-induced endothelial dysfunction in WT but not in the *Lpar5* KO mice. In addition, LPC increased H_2O_2 release from WT vessels, which was significantly reduced in *Lpar5* KO vessels. Our findings indicate that the ATX-LPA-LPA_5 receptor axis is involved in the development of LPC-induced impairment of endothelium-dependent vasorelaxation *via* LPA_5 receptor mediated reactive oxygen species production. Taken together, in this study we identified a new pathway contributing to the development of LPC-induced endothelial dysfunction.

Keywords

Lysophosphatidylcholine, autotaxin, lysophosphatidic acid, lysophosphatidic acid receptor 5, endothelial dysfunction, reactive oxygen species

Impact Statement

The ATX-LPA axis has been proposed to be involved in several cardiovascular diseases; however, its involvement in LPC-induced endothelial dysfunction has not been studied yet. Here we demonstrate for the first time that the development of LPC-induced impairment of endothelium-dependent vasorelaxation requires the conversion of LPC to LPA by the ATX enzyme. LPA activates

LPA_5, triggering signaling pathways that lead to an elevated production of ROS and subsequent endothelial dysfunction. The ATX-LPA-LPA_5 receptor pathway might provide new targets to prevent endothelial dysfunction.

Introduction

Endothelial dysfunction refers to the complex structural and functional alteration of the endothelium that manifests in several cardiovascular diseases including atherosclerosis, diabetes, and hypertension [1]. It is characterized by endothelial cell activation resulting in increased adhesion molecule and cytokine expression and impaired endothelial permeability [2, 3] . The hallmark of endothelial dysfunction is the altered endothelium-dependent vasodilation, mostly attributed to the disrupted synthesis and reduced bioavailability of nitric oxide (NO) [1].

Lysophosphatidylcholine (LPC) is a bioactive glycerophospholipid with well-documented toxic effects on the endothelium [4, 5]. It is present in the circulation in high micromolar concentrations, mostly bound to carrier proteins such as albumin or lipoproteins [6]. LPC is known as a pro-inflammatory mediator that is involved in the progression of several cardiovascular diseases [7]. Moreover, LPC is known to interfere with the NO homeostasis of endothelial cells, that results in an impaired endothelium-dependent vasorelaxation [8, 9].

Although, in the past decades several papers reported the involvement of LPC in the development of endothelial dysfunction, the mechanism underlying this phenomenon remains unclear. Some suggest that LPC might activate signaling pathways that lead to the increased production of reactive oxygen species (ROS) including superoxide and hydrogen peroxide (H_2O_2). These ROS can damage the endothelial cells directly or react with NO reducing the vasorelaxant features of the endothelium [8, 10, 11]. It is also possible that LPC disrupts the integrity of the nitric oxide synthase (NOS) enzyme decreasing its activity [9].

In the vascular system LPC is metabolized by autotaxin (ATX), an ectoenzyme with lysophospholipase D activity, coded by the ectonucleotide pyrophosphatase/phosphodiesterase 2 (ENPP2) gene. ATX is found in the plasma mostly generated by the adipose tissue, but it is also present anchored to the surface of different vascular cells such as the endothelium, smooth muscle, and macrophages. The product of LPC metabolism by ATX is lysophosphatidic acid (LPA), a bioactive

mediator, with multiple vascular functions [12, 13]. Most of the effects of LPA are mediated by six G protein-coupled receptors, that are classified into two groups. LPA_{1-3} are members of the endothelial differentiation gene (EDG) family, whereas LPA_{4-6} are known as non-EDG receptors and share similarities with purinergic receptors [14].

The ATX-LPA-LPA receptor axis has been implicated in the pathology of different inflammatory cardiovascular diseases including atherosclerosis. For example, LPA induces the expression of chemokines and adhesion molecules through activating $LPA_{1/3}$ [15]. In addition, LPA also plays an important role in neointima formation [16, 17]. Despite their documented involvement in progression of vascular dysfunction, the potential role of ATX and LPA in LPC-induced endothelial dysfunction has not yet been reported. In the present study we described the ATX-LPA-LPA_5 axis as a previously unidentified pathway contributing to the LPC-induced impairment of endothelium-dependent vasorelaxation.

Materials and Methods

Animals

All procedures were carried out in accordance with guidelines of the Hungarian Law of Animal Protection (28/1998) and were approved by the Government Office of Pest County (PE/EA/924-7/2021). Wild type (WT) mice on C57BL/6 genetic background were obtained from Charles River Laboratories (Isaszeg, Hungary). Mice deficient in *Lpar1* and *Lpar2* were generated and kindly provided by Dr. Jerold Chun (Sanford Burnham Prebys Medical Discovery Institute, La Jolla, CA, USA). *Lpar4* KO mice were received from Dr. Satoshi Ishii (Department of Immunology, Graduate School of Medicine, Akita University, Akita, Japan) and the *Lpar5* KO animals were a gift from Lexicon Pharmaceuticals (The Woodlands, TX, USA). All transgenic mouse lines had the C57BL/6 genetic background. Animals were housed in a temperature and light controlled room (12 h light-dark cycle) with free access to food and water.

Preparation of vessels

Adult (90-120 days old) male mice were anesthetized in a CO_2-chamber, followed by transcardial perfusion with Krebs solution containing 10 U/mL Heparin as described previously [18]. The thoracic aorta was isolated and cleaned of adipose and connective tissues under dissection microscope (M3Z;

Wild Heerbrugg AG, Gais, Switzerland). During the preparation, special care was taken to preserve the integrity of the endothelium. The distal region of the thoracic aorta was cut into 3 mm long segments and mounted on two parallel stainless-steel needles of a myograph chamber filled with 6 ml gassed Krebs solution at 37°C.

Myography

Before every experiment the vessels were allowed to rest for 45 min at a passive tension of 15 mN. First, the vessels were exposed to 124 mM KCl containing Krebs solution for 1 min to elicit vasoconstriction. After several washes, when the vessels returned to resting tone, phenylephrine (PE) and acetylcholine chloride (ACh) were added to the chambers to test the smooth muscle and the endothelium function. After repeated washing, the segments were adjusted to 124 mM KCl Krebs solution for 3 min to elicit a reference maximal contraction. After washout, the vessels were pre-contracted using increasing concentrations of phenylephrine (10 nM to 10 μM) followed by increasing concentrations of acetylcholine (1 nM to 10 μM) to evoke NO-dependent vasorelaxation. This PE-ACh concentration response curve (CRC) was repeated once more to reach the maximal responsiveness of the rings. After washout, the vessels were treated with 10 μM LPC for 20 min, followed by the readministration of the PE and ACh concentrations. In some experiments, the ATX inhibitor GLPG1690 at 10 μM or 200 U/mL superoxide dismutase (SOD) was applied to the vessels 10 min prior to LPC administration.

Quantification of vascular H_2O_2 release

Whole descending thoracic aortae were cut longitudinally and allowed to rest in 250 μL Hanks' Balanced Salt Solution (HBSS) for 60 min at 37 °C. To measure the basal H_2O_2 levels, the vessels were incubated with a working solution containing 50 μM Amplex Red reagent and 0,2 U/mL horseradish peroxidase (HRP) in HBSS for 15 min at 37 °C. The supernatant was collected and absorbance was measured at 570 nm. Then, the vessels were incubated with working solution containing 10 μM LPC for 40 min at 37 °C followed by absorbance measurement of supernatant. Absorbance values were normalized to 1 min.

Quantitative real-time PCR analysis

Whole thoracic aorta of WT and *Lpar5* KO mice was isolated and stored at -80 °C until RNA isolation. Total RNA from the samples was extracted using Tri Reagent. Total RNA was reverse transcribed using RevertAid First Strand cDNA Synthesis kit. qPCR reactions were performed on CFX Connect Real-Time PCR Detection System (Bio-Rad Laboratories, Hercules, CA, USA) using SsoAdvanced Universal SYBR Green Supermix. Temperature cycles were as follows: 95 °C for 60 s, 95 °C for 10 s and 58 °C for 30 s (40 cycles). Specific primer sets were designed by using Primer3Plus and Primer-BLAST software tools and/or ordered from Sigma-Aldrich.[19, 20] Primer sequences are listed in Table 1. The beta-2 microglobulin (B2m) gene was considered the housekeeping gene for normalizing gene expression. The delta–delta CT (ΔΔCT) method was used to calculate the gene expressions of B2m, LPA_1, LPA_2, LPA_3, LPA_4, LPA_6 receptor and ATX [21]. The minimum information for the publication of quantitative real-time PCR experiments (MIQE) guideline was considered during the entire qPCR quantification workflow and the detailed descriptions of methodology can be found in the Supplementary Materials [22].

Reagents

Oleoyl-lysophosphatidylcholine (18:1 LPC) was purchased from Sigma-Aldrich (St. Louis, MO, USA) and was dissolved in methanol to stock solutions of 10 mM. Required amounts of LPC stock solutions were transferred to glass vials and the vehicle was removed using a stream of nitrogen. LPC was re-dissolved in water containing 0,1% bovine serum albumin before use. SOD was also purchased from Sigma Aldrich and dissolved in water to stock solutions of 20000 U/mL. GLPG1690 was purchased from Cayman Chemicals (Ann Arbor, MI, USA) and DMSO was used as a solvent for preparing a 10 mM stock solution. Amplex™ Red reagent and HRP were purchased from Thermo Fisher Scientific (Waltham, MA, USA) and were diluted in DMSO and aqueous solutions to stock solutions of 10 mM and 0.4 U/mL. Tri Reagent was purchased from Zymo Research (Irvine, CA, USA). RevertAid First Strand cDNA Synthesis kit was purchased from Thermo Scientific (Waltham, MA, USA). SsoAdvanced Universal SYBR Green Supermix was purchased from Bio-Rad Laboratories (Hercules, CA, USA).

Data analysis

Vascular tension changes were recorded with the MP100 system and analyzed with the AcqKnowledge 3.7.3 software of Biopac System Inc. (Goleta, CA, USA). All data are presented as mean ± SE, and 'n' demonstrates the number of vessels tested. Data analysis was carried out by GraphPad Prism statistical software (version 8.0.1.244; GraphPad Software Inc., La Jolla, CA, USA). Concentration-response curves for ACh were plotted with responses expressed as percentage of the maximal contraction induced by PE. Nonlinear regression was fitted to compare the dose-response curves and determine E_{max} and EC50 values. Student's t-test or Mann-Whitney test was used when comparing two variables. $p<0.05$ was considered statistically significant.

Results

Inhibition of ATX attenuates LPC-induced endothelial dysfunction

LPC reportedly evokes endothelial dysfunction characterized by reduction in NO-dependent vasorelaxation [10]. In agreement with that, we observed that in LPC treated WT vessels, the ACh-induced vasorelaxant responses were markedly attenuated (Figure 1). To investigate the contribution of ATX to this deleterious effect of LPC, vessels were pre-treated with the selective ATX inhibitor GLPG1690. GLPG1690 significantly ($p<0.0001$) decreased the LPC-induced endothelial dysfunction (Figure 1), suggesting the involvement of ATX in the effect of LPC.

Identification of LPA receptors involved in LPC-induced endothelial dysfunction

Because ATX appeared to be involved in the LPC-induced attenuation of endothelial function, we examined whether its product, LPA also contributes to the effect. Therefore, the effect of LPC was tested on aorta segments isolated from mice KO for different LPA receptors. In the case of *Lpar1, Lpar2* and *Lpar4* KO, the effect of LPC was similar to that observed in WT mice (Figure 2A-C). On the contrary, the impairment of ACh-induced vasorelaxation by LPC was markedly attenuated in *Lpar5* KO mice (Figure 2D). These results indicate that LPC-derived LPA may contribute to the development of endothelial dysfunction through LPA_5 receptor activation.

Expression profile of LPA receptors and ATX in *Lpar5* KO mice

We examined the LPA receptor and ATX expression profile in aortic tissue isolated from WT and *Lpar5* KO mice using quantitative real-time PCR. Our data showed that *Lpar5* deletion did not

significantly affect the expression of LPA_1, LPA_2, LPA_3, LPA_4, LPA_6 receptors and ATX as no significant differences in mRNA expression rate were detected relative to WT (Figure 3).

Involvement of ROS in LPC-induced endothelial dysfunction

In the next phase of the study, we investigated the downstream signaling mechanism involved in the LPA receptor-mediated portion of the LPC-induced endothelial dysfunction. Considering that superoxide is a well-known factor participating in the development of endothelial dysfunction [1], we tested the effect of SOD on the deleterious effect of LPC. As shown in Figure 4A, SOD prevented the effect of LPC treatment in WT vessels. Interestingly, this beneficial effect of SOD was absent in *Lpar5* KO vessels (Figure 4B), indicating that LPA_5 drives ROS production.

To confirm the involvement of LPA_5 receptor in ROS generation upon LPC treatment, H_2O_2 production assay was performed in the vessels. LPC induced a marked increase in extracellular H_2O_2 levels in aortic tissue isolated from WT mice, however, its effect was significantly ($p<0.05$) diminished in *Lpar5* KO vessels (Figure 5). These data suggest that the LPA_5 activation is involved in LPC-evoked ROS production.

Discussion

In the present study, we demonstrated that ATX and LPA_5 receptor contribute to the LPC-induced impairment of endothelium-dependent vasorelaxation. Furthermore, these results suggest that the reduction of NO-dependent vasorelaxation is coupled with elevated ROS production and this effect is mediated, at least in part by LPA_5 activation.

Although ATX and LPA are associated reportedly with inflammatory vascular diseases like atherosclerosis [16, 23], their involvement in the alteration of endothelium-dependent vasorelaxation has not yet been investigated. In contrast, the disruptive effect of LPC on vasorelaxation is well-documented [8, 10, 11]; however, to the best of our knowledge the potential involvement of ATX and LPA in this process has not been addressed previously. Here we demonstrated that the selective inhibition of ATX significantly reduces the LPC-induced impairment of endothelial function, suggesting that LPC achieves this effect partly by conversion to LPA.

The involvement of LPA was further confirmed, as we observed that the deletion of *Lpar5* is protective of the LPC-evoked endothelial dysfunction. Since its discovery in 2006 [24], LPA_5 receptor

has been implicated in multiple biological functions such as brain development [25], immune modulation [26] and neuropathic pain sensitization [27]. In the vascular system LPA_5 is expressed in endothelial cells [28], smooth muscle cells [29] and platelets [30]. LPA_5 has also been associated with atherosclerosis progression, as its expression was found to be upregulated in atherosclerotic plaques isolated from human carotid arteries [31]. It has been assumed that LPA_5 along with other LPA receptors is involved in endothelial cell activation [31], which further supports our hypothesis that LPA_5 is a potential regulator of vascular inflammatory processes.

We also analyzed the LPA receptor and ATX expression profile of WT and *Lpar5* KO mice. The results showed no significant difference between the two groups suggesting that the genetic deletion of LPA_5 does not affect the expression of other LPA receptors and ATX.

The deleterious effects of LPC on endothelial cells are well documented and mostly attributed to the ability of LPC to evoke oxidative stress. Several research groups reported increased ROS production in cultured endothelial cells upon LPC treatment [8, 32]. The release of these oxidative agents can contribute to the disruption of the normal endothelial function, leading to decreased endothelium-dependent vasorelaxation [10]. As Rao et al. showed earlier [10], the negative effect of 18:1 LPC on NO-dependent vasorelaxation can be almost entirely abolished by the superoxide-scavenger Tempol. Our results are in agreement with these observations, as SOD enzyme significantly decreased LPC evoked attenuation of vasorelaxation in WT mice, albeit its protective effect was not complete. One possible explanation for this difference is that while Tempol is a membrane-permeable agent, reacting with both intracellular and extracellular ROS [33], SOD has poor membrane permeability and acts extracellularly [34]. The involvement of extracellular ROS in this phenomenon was further confirmed by the results we obtained in the Amplex Red assay, a method used for extracellular H_2O_2 detection [35]. In the supernatant of LPC treated WT vessels, a significant amount of H_2O_2 was detected, indicating that LPC evokes ROS release from vascular cells. Interestingly, in case of *Lpar5* KO vessels, we could not achieve further improvement with SOD treatment. In addition, we observed significantly lower ROS release upon LPC stimulation in *Lpar5* KO as compared to WT vessels. These results indicate that LPA_5 receptor activation is involved in the initiation of oxidative stress in mouse aortic tissue.

Whereas our results suggest that a significant part of the deleterious effect of LPC requires its conversion to LPA, it is likely that other, LPA-independent signaling pathways are also involved, as we were unable to prevent the entire LPC effect either with ATX inhibition or the genetic deletion of LPA_5. Given its amphipathic nature, it is likely that LPC interacts directly with the cell membrane, changing its biophysical properties leading to an altered membrane function [36]. In line with this hypothesis, it has been speculated that LPC might incorporate into the endothelial cell membrane and interacts with the eNOS enzymes located in caveolae [8, 37] This process may lead to a disrupted eNOS function with decreased NO bioavailability and subsequent endothelial dysfunction.

In conclusion, we have shown that the development of LPC-induced impairment of endothelium-dependent vasorelaxation requires the conversion of LPC to LPA by the ATX enzyme in mouse aortic tissue. This locally formed LPA appears to activate LPA_5 receptor, triggering signaling pathways that lead to an elevated production of ROS and subsequent endothelial dysfunction.

Authors' Contributions

A.J., A.M., M.K., M.G., G.J.T., Z.B. and É.R. conceived and designed research, J.C. and S.I. provided LPA receptor knock-out mice, A.J., A.M., M.K. and É.R. performed experiments, A.J. and A.M. analyzed data, A.J. prepared figures, A.J. drafted manuscript, A.J., A.M., M.K., M.G., J.C., S.I., G.J.T., Z.B. and É.R. edited and revised manuscript, A.J., A.M., M.K., M.G., J.C., S.I., G.J.T., Z.B. and É.R. approved final version of manuscript.

Acknowledgements

The authors are grateful to Margit Kerék, Ildikó Murányi, Balázs Besztercei and Ágnes Fülöp for their technical assistance.

Conflict of Interest

The authors declared no potential conflicts of interest with respect to the research, authorship, and/or publication of this article.

Funding

This work was supported by the Hungarian National Research, Development and Innovation Office [K-125174, PD-132851, K-135683, K-139230, NVKP_16-1-2016-0042, EFOP-3.6.3-VEKOP-16-

2017-00009] and by the Ministry for Innovation and Technology from the Hungarian NRDI Fund [2020-1.1.6-JÖVŐ-2021-00010; 2020-1.1.6-JÖVŐ-2021-00013; TKP2021-EGA-25].

Figure Legends

Figure 1. Cumulative concentration-response curves to ACh were performed on WT mouse aortic rings before and after incubation with 18:1 LPC (10 μM, 20 min) in the presence or absence of GLPG1690, a selective ATX inhibitor (10 μM). GLPG1690 significantly reduced the LPC-evoked attenuation of vasorelaxation. Relaxation values are expressed as mean ± SE percentage of maximal PE-induced contraction. LPC: n=31, GLPG+LPC: n=38. *p<0.0001 compared to "After GLPG+LPC".

Figure 2. Cumulative concentration-response curves to ACh were performed on aortic rings before and after incubation with 18:1 LPC (10 μM, 20 min). Vessels were isolated from *Lpar1* (A), *Lpar2* (B), *Lpar4* (C), *Lpar5* (D) KO and WT mice. The LPC-induced attenuation of endothelium-dependent vasorelaxation was unaltered in *Lpar1* (A), *Lpar2* (B), and *Lpar4* (C) KO, but it was reduced in *Lpar5* KO (D). Relaxation values represent mean ± SE percentage of maximal PE-induced contraction. A: WT: n=15, KO: n=13. B: WT: n=9, KO: n=9. C: WT: n=10, KO: n=14. D: WT: n=49, KO: n=60. *p<0.0001 compared to "KO After LPC".

Figure 3. LPA receptor and ATX expression of mouse aortic tissue isolated from WT (grey bars) and *Lpar5* KO (red bars) mice. mRNA expression was determined using quantitative real-time PCR. No statistical difference was observed in LPA_1, LPA_2, LPA_3, LPA_4, LPA_6 receptors and ATX gene expression between the two groups. The changes in mRNA expression of examined genes were normalized to B2m mRNA levels. LPA_1: Bl6: n=8, *Lpar5* KO: n=8. LPA_2: Bl6: n=6, *Lpar5* KO: n=6. LPA_3: Bl6: n=7, *Lpar5* KO: n=6. LPA_4: Bl6: n=8, *Lpar5* KO: n=8. LPA_6: Bl6: n=9, *Lpar5* KO: n=8. ATX: Bl6: n=9, *Lpar5* KO: n=8. Student's t-test, Mann-Whitney test.

Figure 4. Cumulative concentration-response curves to ACh were performed on aortic rings before and after incubation with 18:1 LPC (10 μM, 20 min) in the presence or absence of SOD (200 U/ml). Vessels were isolated from WT (A) or *Lpar5* KO (B) mice. SOD significantly reduced the LPC-evoked attenuation of vasorelaxation in WT (A), but it was ineffective in *Lpar5* KO (B). Relaxation

values represent mean ± SE percentage of maximal PE-induced contraction. A: LPC: n=29, SOD+LPC: n=30. B: LPC: n=9, SOD+LPC: n=9. *p<0.0001 compared to "After SOD+LPC".

Figure 5. H_2O_2 production of WT (gray bar) and *Lpar5* KO (red bar) mouse aortic rings measured by Amplex Red Assay. Vessels were incubated with working solution containing Amplex Red (50 μM) and HRP (0,2 U/mL) in HBSS at 37 °C. Absorbance was measured from supernatant after 15 min. Then, the vessels were incubated with working solution containing 18:1 LPC (10 μM) for 40 min at 37 °C followed by absorbance measurement of supernatant. The LPC-evoked H_2O_2 production was significantly reduced in *Lpar5* KO as compared to WT vessels. Absorbance values were normalized to 1 min. Values are expressed as fold H_2O_2 increase after LPC treatment. WT: n=9, *Lpar5* KO: n=6. *p<0.05 compared to *Lpar5* KO. Mann-Whitney test.

References

1. Vanhoutte PM, Shimokawa H, Tang EH, Feletou M. Endothelial dysfunction and vascular disease. *Acta Physiol (Oxf)* 2009;**196**:193-222

2. De Meyer GR, Herman AG. Vascular endothelial dysfunction. *Prog Cardiovasc Dis* 1997;**39**:325-42

3. Davignon J, Ganz P. Role of endothelial dysfunction in atherosclerosis. *Circulation* 2004;**109**:III27-32

4. Kume N, Cybulsky MI, Gimbrone MA, Jr. Lysophosphatidylcholine, a component of atherogenic lipoproteins, induces mononuclear leukocyte adhesion molecules in cultured human and rabbit arterial endothelial cells. *J Clin Invest* 1992;**90**:1138-44

5. Huang F, Subbaiah PV, Holian O, Zhang J, Johnson A, Gertzberg N, Lum H. Lysophosphatidylcholine increases endothelial permeability: role of PKCalpha and RhoA cross talk. *Am J Physiol Lung Cell Mol Physiol* 2005;**289**:L176-85

6. Croset M, Brossard N, Polette A, Lagarde M. Characterization of plasma unsaturated lysophosphatidylcholines in human and rat. *Biochem J* 2000;**345 Pt 1**:61-7

7. Law SH, Chan ML, Marathe GK, Parveen F, Chen CH, Ke LY. An Updated Review of Lysophosphatidylcholine Metabolism in Human Diseases. *Int J Mol Sci* 2019;**20**:1149

8. Kozina A, Opresnik S, Wong MS, Hallstrom S, Graier WF, Malli R, Schroder K, Schmidt K, Frank S. Oleoyl-lysophosphatidylcholine limits endothelial nitric oxide bioavailability by induction of reactive oxygen species. *PLoS One* 2014;**9**:e113443

9. Campos-Mota GP, Navia-Pelaez JM, Araujo-Souza JC, Stergiopulos N, Capettini LSA. Role of ERK1/2 activation and nNOS uncoupling on endothelial dysfunction induced by lysophosphatidylcholine. *Atherosclerosis* 2017;**258**:108-18

10. Rao SP, Riederer M, Lechleitner M, Hermansson M, Desoye G, Hallstrom S, Graier WF, Frank S. Acyl chain-dependent effect of lysophosphatidylcholine on endothelium-dependent vasorelaxation. *PLoS One* 2013;**8**:e65155

11. Safaya R, Chai H, Kougias P, Lin P, Lumsden A, Yao Q, Chen C. Effect of lysophosphatidylcholine on vasomotor functions of porcine coronary arteries. *J Surg Res* 2005;**126**:182-8

12. Zhao Y, Hasse S, Zhao C, Bourgoin SG. Targeting the autotaxin - Lysophosphatidic acid receptor axis in cardiovascular diseases. *Biochem Pharmacol* 2019;**164**:74-81

13. Moolenaar WH, Perrakis A. Insights into autotaxin: how to produce and present a lipid mediator. *Nat Rev Mol Cell Biol* 2011;**12**:674-9

14. Geraldo LHM, Spohr T, Amaral RFD, Fonseca A, Garcia C, Mendes FA, Freitas C, dosSantos MF, Lima FRS. Role of lysophosphatidic acid and its receptors in health and disease: novel therapeutic strategies. *Signal Transduct Target Ther* 2021;**6**:45

15. Lin CI, Chen CN, Lin PW, Chang KJ, Hsieh FJ, Lee H. Lysophosphatidic acid regulates inflammation-related genes in human endothelial cells through LPA1 and LPA3. *Biochem Biophys Res Commun* 2007;**363**:1001-8

16. Hao F, Zhang F, Wu DD, An D, Shi J, Li G, Xu X, Cui MZ. Lysophosphatidic acid-induced vascular neointimal formation in mouse carotid arteries is mediated by the matricellular protein CCN1/Cyr61. *Am J Physiol Cell Physiol* 2016;**311**:C975-C84

17. Cheng Y, Makarova N, Tsukahara R, Guo H, Shuyu E, Farrar P, Balazs L, Zhang C, Tigyi G. Lysophosphatidic acid-induced arterial wall remodeling: requirement of PPARgamma but not LPA1 or LPA2 GPCR. *Cell Signal* 2009;**21**:1874-84

18. Horvath B, Orsy P, Benyo Z. Endothelial NOS-mediated relaxations of isolated thoracic aorta of the C57BL/6J mouse: a methodological study. *J Cardiovasc Pharmacol* 2005;**45**:225-31

19. Untergasser A, Cutcutache I, Koressaar T, Ye J, Faircloth BC, Remm M, Rozen SG. Primer3--new capabilities and interfaces. *Nucleic Acids Res* 2012;**40**:e115

20. Ye J, Coulouris G, Zaretskaya I, Cutcutache I, Rozen S, Madden TL. Primer-BLAST: a tool to design target-specific primers for polymerase chain reaction. *BMC Bioinformatics* 2012;**13**:134

21. Pfaffl MW. A new mathematical model for relative quantification in real-time RT-PCR. *Nucleic Acids Res* 2001;**29**:e45

22. Bustin SA, Benes V, Garson JA, Hellemans J, Huggett J, Kubista M, Mueller R, Nolan T, Pfaffl MW, Shipley GL, Vandesompele J, Wittwer CT. The MIQE guidelines: minimum information for publication of quantitative real-time PCR experiments. *Clin Chem* 2009;**55**:611-22

23. Karshovska E, Mohibullah R, Zhu M, Zahedi F, Thomas D, Magkrioti C, Geissler C, Megens RTA, Bianchini M, Nazari-Jahantigh M, Ferreiros N, Aidinis V, Schober A. Endothelial ENPP2 (Ectonucleotide Pyrophosphatase/Phosphodiesterase 2) Increases Atherosclerosis in Female and Male Mice. *Arterioscler Thromb Vasc Biol* 2022;**42**:1023-36

24. Lee CW, Rivera R, Gardell S, Dubin AE, Chun J. GPR92 as a new G12/13- and Gq-coupled lysophosphatidic acid receptor that increases cAMP, LPA5. *J Biol Chem* 2006;**281**:23589-97

25. Ohuchi H, Hamada A, Matsuda H, Takagi A, Tanaka M, Aoki J, Arai H, Noji S. Expression patterns of the lysophospholipid receptor genes during mouse early development. *Dev Dyn* 2008;**237**:3280-94

26. Mathew D, Kremer KN, Strauch P, Tigyi G, Pelanda R, Torres RM. LPA(5) Is an Inhibitory Receptor That Suppresses CD8 T-Cell Cytotoxic Function via Disruption of Early TCR Signaling. *Front Immunol* 2019;**10**:1159

27. Lin ME, Rivera RR, Chun J. Targeted deletion of LPA5 identifies novel roles for lysophosphatidic acid signaling in development of neuropathic pain. *J Biol Chem* 2012;**287**:17608-17

28. Ruisanchez E, Dancs P, Kerek M, Nemeth T, Farago B, Balogh A, Patil R, Jennings BL, Liliom K, Malik KU, Smrcka AV, Tigyi G, Benyo Z. Lysophosphatidic acid induces vasodilation mediated by LPA1 receptors, phospholipase C, and endothelial nitric oxide synthase. *FASEB J* 2014;**28**:880-90

29. Dancs PT, Ruisanchez E, Balogh A, Panta CR, Miklos Z, Nusing RM, Aoki J, Chun J, Offermanns S, Tigyi G, Benyo Z. LPA(1) receptor-mediated thromboxane A(2) release is responsible for lysophosphatidic acid-induced vascular smooth muscle contraction. *FASEB J* 2017;**31**:1547-55

30. Khandoga AL, Fujiwara Y, Goyal P, Pandey D, Tsukahara R, Bolen A, Guo H, Wilke N, Liu J, Valentine WJ, Durgam GG, Miller DD, Jiang G, Prestwich GD, Tigyi G, Siess W. Lysophosphatidic acid-induced platelet shape change revealed through LPA(1-5) receptor-selective probes and albumin. *Platelets* 2008;**19**:415-27

31. Aldi S, Matic LP, Hamm G, van Keulen D, Tempel D, Holmstrom K, Szwajda A, Nielsen BS, Emilsson V, Ait-Belkacem R, Lengquist M, Paulsson-Berne G, Eriksson P, Lindeman JHN, Gool AJ, Stauber J, Hedin U, Hurt-Camejo E. Integrated Human Evaluation of the Lysophosphatidic Acid Pathway as a Novel Therapeutic Target in Atherosclerosis. *Mol Ther Methods Clin Dev* 2018;**10**:17-28

32. da Silva JF, Alves JV, Silva-Neto JA, Costa RM, Neves KB, Alves-Lopes R, Carmargo LL, Rios FJ, Montezano AC, Touyz RM, Tostes RC. Lysophosphatidylcholine induces oxidative stress in human endothelial cells via NOX5 activation - implications in atherosclerosis. *Clin Sci (Lond)* 2021;**135**:1845-58

33. Simonsen U, Christensen FH, Buus NH. The effect of tempol on endothelium-dependent vasodilatation and blood pressure. *Pharmacol Ther* 2009;**122**:109-24

34. Beckman JS, Minor RL, Jr., White CW, Repine JE, Rosen GM, Freeman BA. Superoxide dismutase and catalase conjugated to polyethylene glycol increases endothelial enzyme activity and oxidant resistance. *J Biol Chem* 1988;**263**:6884-92

35. Dikalov S, Griendling KK, Harrison DG. Measurement of reactive oxygen species in cardiovascular studies. *Hypertension* 2007;**49**:717-27

36. Leung YM, Xion Y, Ou YJ, Kwan CY. Perturbation by lysophosphatidylcholine of membrane permeability in cultured vascular smooth muscle and endothelial cells. *Life Sci* 1998;**63**:965-73

37. Stoll LL, Oskarsson HJ, Spector AA. Interaction of lysophosphatidylcholine with aortic endothelial cells. *Am J Physiol* 1992;**262**:H1853-60

Gene name	Primer sequence	NCBI reference sequence number	Size (bp)	Reference
Target genes				
Lpar1 (lysophosphatidic acid receptor 1)	F: GACTCCTACTTAGTCTTCTGG R: CAGACAATAAAGGCACCAAG	NM_010336.2	200	Purchased from Sigma-Aldrich
Lpar2 (lysophosphatidic acid receptor 2)	F: CAAGACGGTTGTCATCATTC R: AATATACCACTGCATTGACC	NM_020028.3	167	
Lpar3 (lysophosphatidic acid receptor 3)	F: AGGGCTCCCATGAAGCTAAT R: GTTGCACGTTACACTGCTTG	NM_022983.4	124	[20]
Lpar4 (lysophosphatidic acid receptor 4)	F: CTGATCGTCTGCCTCCAGAAA R: TTGAGACTGAGGACCAGTAGAG	NM_175271.4	117	[20]
Lpar6 (lysophosphatidic acid receptor 6)	F: ACTGAAGTAAAGCTGGTTTG R: AACCCATAAAGCTGAAAGTG	NM_175116.4	109	Purchased from Sigma-Aldrich
Enpp2 (ectonucleotide pyrophosphatase/ phosphodiesterase 2)	F: CTGTCTTTGATGCTACTTTCC R: TCACAGACCAAAAGAATGTC	NM_001040092.3	129	
Reference gene				
B2m (beta-2 microglobulin)	F: CTTTCTGGTGCTTGTCTCACTG R: AGTATGTTCGGCTTCCCATTC	NM_009735.3	105	[19]

Table 1. Primer sequences used in quantitative PCR analysis

The gene identities and forward (F) and reverse (R) primer sequences with the length of the PCR products for qPCR. The specific PCR products were checked by gel electrophoresis for absence of primer-dimers and correct PCR product length.

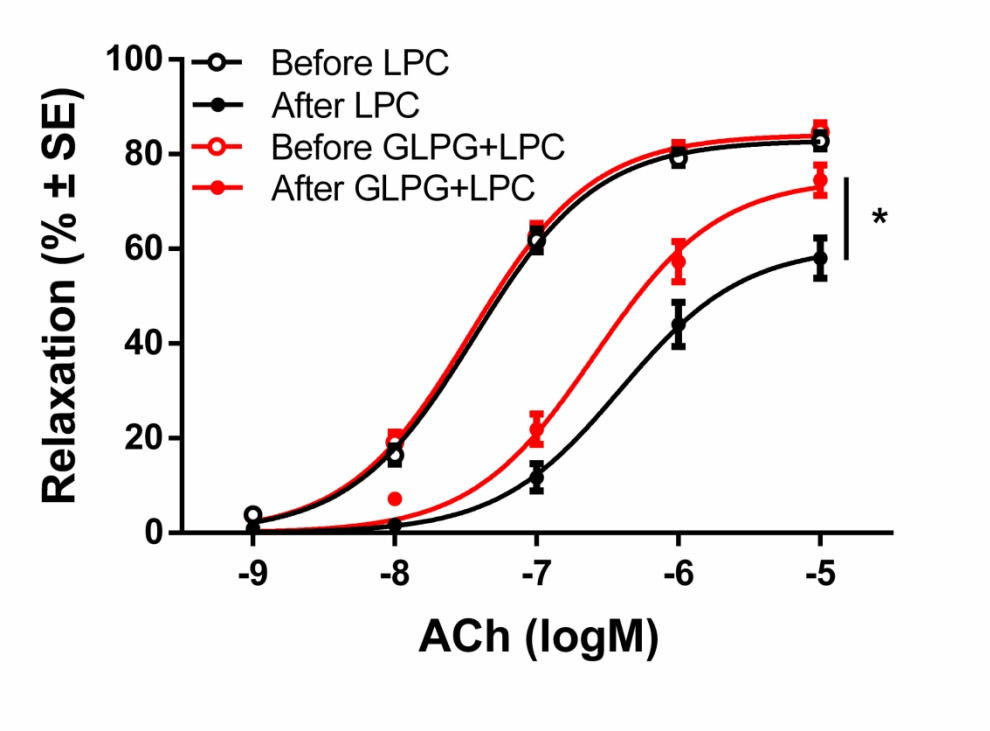

Figure 1. Involvement of ATX in LPC-induced endothelial dysfunction

107x79mm (600 x 600 DPI)

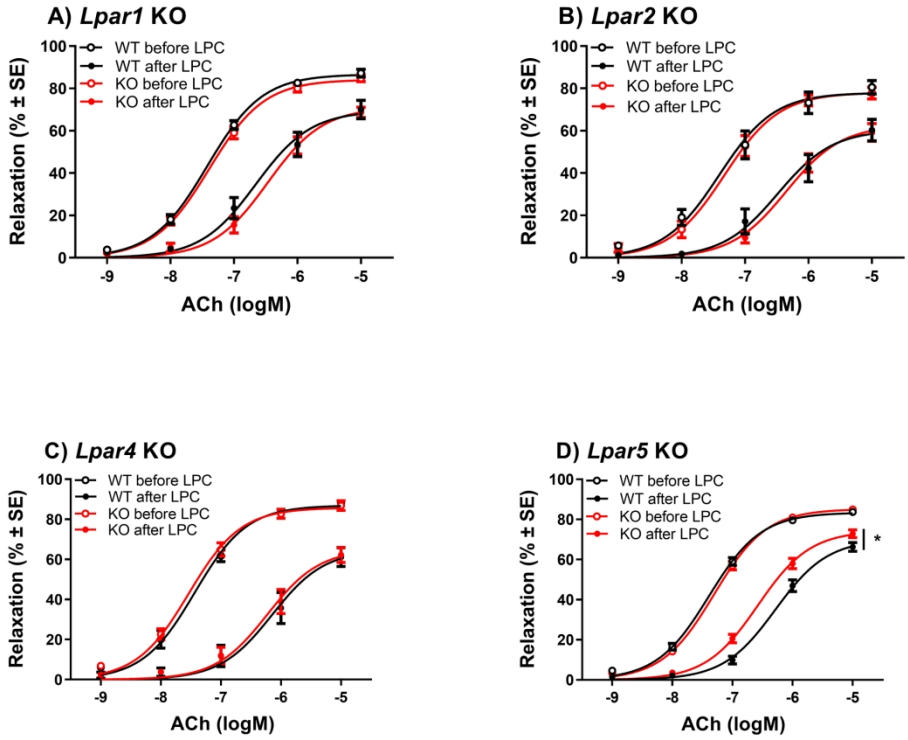

Figure 2. Identification of LPA receptors involved in LPC-induced endothelial dysfunction

196x161mm (300 x 300 DPI)

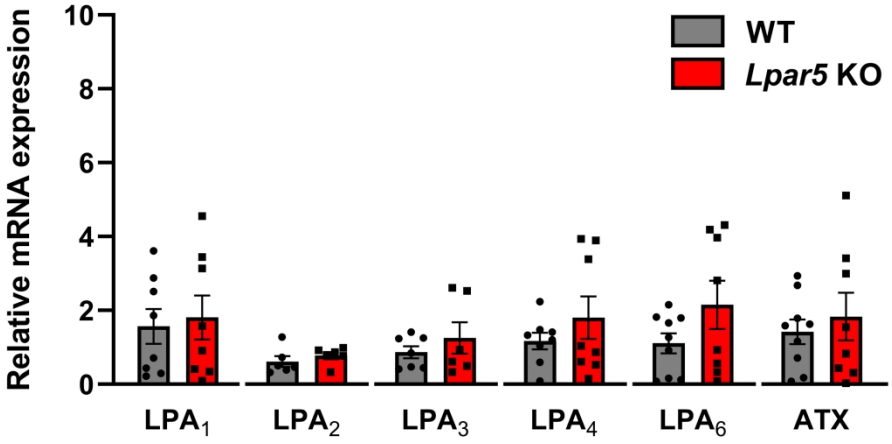

Figure 3. Expression profile of LPA receptors and ATX in *Lpar5* KO mice

137x65mm (600 x 600 DPI)

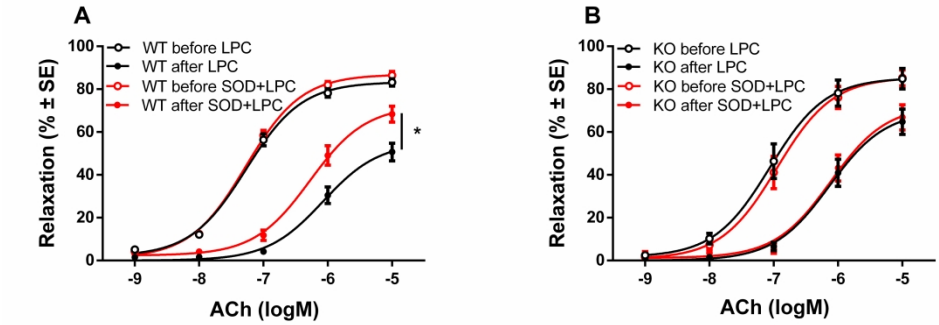

Figure 4. Involvement of ROS in LPC-induced endothelial dysfunction

196x79mm (600 x 600 DPI)

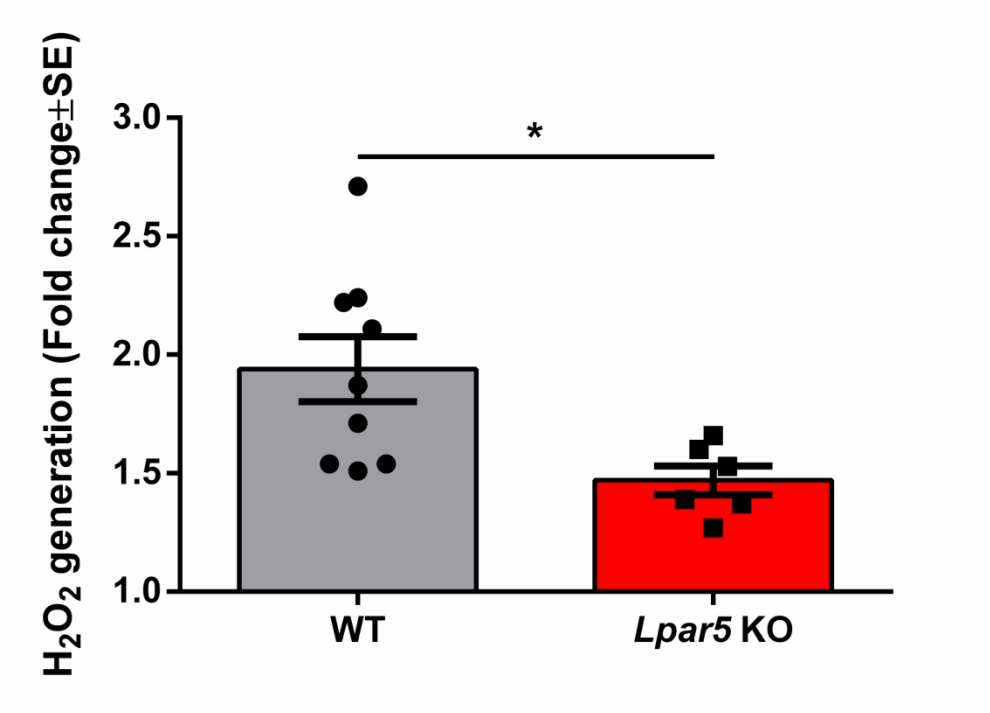

Figure 5. Involvement of LPA_5 receptor in LPC-evoked ROS release

107x76mm (600 x 600 DPI)

Assessment of gene expression

Thoracic aorta of WT and *Lpar5* KO mice was isolated and stored at -80 °C until PCR analysis. Thoracic aorta samples were homogenized (Capitol Scientific, BEL-19923-0000) and subsequently lysed in 0.5 ml Tri Reagent (Zymo Research, R2050-1-50). A total of 0.2 ml chloroform (Reanal Laborvegyszer Kft) was added per 1 ml Tri Reagent, the samples were mixed for 15 s by vigorous shaking. Phase separation was allowed by placing the samples to room temperature for 15 min followed by centrifugation at 12,000 ×*g* for 15 min at 4°C. The upper aqueous phase was transferred to a fresh tube. A total of 0.5 ml isopropanol (Thermo Scientific, 59304) per 1 ml Tri Reagent was added, thoroughly mixed, and incubated for 10 min and centrifuged at 12,000 ×*g* for 10 min at 4°C to precipitate the RNA. The RNA pellet was washed with 2 ml ethanol (Molar Chemicals Ktf) per 1 ml Tri reagent and centrifugation at 12,000 ×*g* for 8 min at 4°C. The supernatant was aspirated and the sediment was air dried. Total RNA was dissolved in UltraPure water (Invitrogen, 10977015) and RNA quantity and purity of all samples were measured with NanoDrop spectrophotometer (Thermo Scientific). Total RNA samples were stored at −80 °C until use.

Total RNA was reverse transcribed using RevertAid First Strand cDNA Synthesis kit (Thermo Scientific, K1621) and Bio-Rad C1000 Touch PCR thermal cycler. Reverse transcription was carried out according to the manufacturer's instructions using the following temperature cycles: 25 °C for 5 min, 42 °C for 60 min and 70 °C for 5 min. The cDNA was stored at −20 °C.

Specific primer sets were designed by using Primer3Plus (https://www.primer3plus.com/) and Primer-BLAST software tool (http://www.ncbi.nlm.nih.gov/tools/primer-blast) and/or ordered from Sigma-Aldrich [1, 2]. Primer sequences are listed in Table 1. qPCR reactions were performed on CFX Connect Real-Time PCR Detection System (Bio-Rad Laboratories) using SsoAdvanced Universal SYBR Green Supermix (Bio-Rad Laboratories). The sample volume was 10 µl containing 2 µl diluted cDNA, 1 µl forward and 1 µl reverse primer (0.5-0.5 µM), 5 µl SsoAdvanced Universal SYBR Green Supermix and UltraPure water (Invitrogen, 10977015). PCR reactions were carried out in triplicate. Temperature cycle were as follows: 95 °C for 60 s, 95 °C for 10 s and 58 °C for 30 s (40 cycles), followed by a melting curve analysis by heating from 65°C to 95°C with a rate of 0.5°C/s and continuous fluorescence

measurement. Raw data were analyzed using CFX Maestro Software 2.2 software (Bio-Rad Laboratories).

Data evaluation, statistical analysis and graphs were performed with GrapPadPrism 8 (GraphPad Software, version 8.0.1.244) with n= 6-9 independent repetitions. The Pfaffl method, also known as the delta–delta CT (ΔΔCT) method, with efficiency correction was used to calculate the gene expressions of beta-2 microglobulin (B2m), LPA_1, LPA_2, LPA_3, LPA_4, LPA_6 receptor and ATX [3, 4]. B2m was considered the housekeeping gene for normalising gene expression. For B2m, efficiency was 1.13; for Lpar1 1.11; for Lpar2 1.10; for Lpar3 0.80; for Lpar4 0.83; for Lpar6 1.08; for Enpp2, efficiency was 1.12. Normal distribution was analyzed with the Shapiro-Wilk test. Differences between different conditions were calculated by unpaired Student's t-test. Nonparametric values were analyzed with Mann-Whitney U test. p values ≤ 0.05 were considered statistically significant, all experimental data are shown as means ± SE (n = 6–9). The minimum information for the publication of quantitative real-time PCR experiments (MIQE) guidelines was considered during the entire qPCR quantification workflow [4].

References

1. Untergasser A, Cutcutache I, Koressaar T, Ye J, Faircloth BC, Remm M, Rozen SG. Primer3--new capabilities and interfaces. *Nucleic Acids Res* 2012;**40**:e115

2. Ye J, Coulouris G, Zaretskaya I, Cutcutache I, Rozen S, Madden TL. Primer-BLAST: a tool to design target-specific primers for polymerase chain reaction. *BMC Bioinformatics* 2012;**13**:134

3. Pfaffl MW. A new mathematical model for relative quantification in real-time RT-PCR. *Nucleic Acids Res* 2001;**29**:e45

4. Bustin SA, Benes V, Garson JA, Hellemans J, Huggett J, Kubista M, Mueller R, Nolan T, Pfaffl MW, Shipley GL, Vandesompele J, Wittwer CT. The MIQE guidelines: minimum information for publication of quantitative real-time PCR experiments. *Clin Chem* 2009;**55**:611-22

International Journal of
Molecular Sciences

MDPI

Article

Enhancement of sphingomyelinase-induced endothelial nitric oxide synthase-mediated vasorelaxation in a murine model of type 2 diabetes

Éva Ruisanchez [1,2], Rita Cecília Panta [1], Anna Janovicz [1,2], Levente Kiss [3], Adrienn Párkányi [1], Zsuzsa Straky [1], Dávid Korda [1], Károly Liliom [4], Gábor Tigyi [1,5] and Zoltán Benyó [1,2]*

[1] Institute of Translational Medicine, Semmelweis University, Budapest, Hungary

[2] Eötvös Loránd Research Network and Semmelweis University (ELKH-SE) Cerebrovascular and Neurocognitive Disorders Research Group, Budapest, Hungary

[3] Department of Physiology, Semmelweis University, Budapest, Hungary

[4] Institute of Biophysics and Radiation Biology, Semmelweis University, Budapest, Hungary

[5] Department of Physiology, University of Tennessee Health Science Center, Memphis, Tennessee, United States of America

* Correspondence: benyo.zoltan@med.semmelweis-univ.hu.

Citation: Ruisanchez, É.; Panta, R.C.; Janovicz, A.; Kiss, L.; Párkányi, A.; Straky, Z.; Korda, D.; Liliom, K.; Tigyi, G.; Benyó, Z. Enhancement of sphingomyelinase-induced endothelial nitric oxide synthase-mediated vasorelaxation in a murine model of type 2 diabetes**.** *Int. J. Mol. Sci.* **2023**, *23*, x. https://doi.org/10.3390/xxxxx

Academic Editor(s):

Received: date
Accepted: date

Published: date

Abstract: (1) Background: Sphingolipids are important biological mediators both in health and in metabolic diseases. We investigated the vascular effects of enhanced sphingomyelinase (SMase) activity in a mouse model of type 2 diabetes mellitus (T2DM) to gain understanding of the secondary signaling pathways involved.; (2) Methods: wire myography was used to measure isometric changes in the tone of the thoracic aorta after administration of 0.2 U/ml neutral SMase in the presence or absence of the thromboxane prostanoid (TP) receptor antagonist SQ 29,548 and nitric oxide synthase (NOS) inhibitor L-NAME; (3) Results: In phenylephrine-precontracted aortic segments of non-diabetic mice, 0.2 U/mL neutral SMase induced transient contraction and subsequent weak relaxation, whereas vessels of littermate adult male diabetic (Leprdb/Leprdb, referred to as db/db) mice showed marked relaxation. In the presence of the TP receptor antagonist SQ 29,548, SMase induced enhanced relaxation in both groups, which was 3-fold stronger in vessels of db/db mice as compared to controls. Co-administration of the NOS inhibitor L-NAME abolished the vasorelaxation in both groups; (4) Conclusions: Our results indicate dual vasoactive effects of SMase: TP-mediated vasoconstriction and NO-mediated vasorelaxation. Surprisingly, in spite of the general endothelial dysfunction in T2DM, the endothelial NOS-mediated vasorelaxant effect of SMase was markedly enhanced.

Keywords: Sphingolipids; sphingomyelinase; vasorelaxation; endothelial nitric oxide synthase; type 2 diabetes; thromboxane prostanoid receptor

1. Introduction

Sphingolipids, derived from sphingomyelin metabolism, have been implicated as important mediators in the physiology and pathophysiology of the car-

diovascular system [1-6]. Sphingomyelinase (SMase) catalyzes the conversion of sphingomyelin to ceramide, which is the precursor of other sphingolipid mediators, including ceramide-1-phosphate (C1P), sphingosine (Sph), and sphingosine-1-phosphate (S1P) [7]. The majority of S1P-induced biological effects are mediated by G-protein-coupled receptors (GPCRs), termed $S1P_{1-5}$ [8]. Other sphingolipid mediators may exert biological effects by directly interacting with membrane or intracellular protein targets, independently of the activation of S1P receptors [5,9-11].

Based on the optimal pH for their catalytic activity, SMase isoforms can be divided into three groups: alkaline, acidic, and neutral [12]. The expression and known functions of alkaline SMase are mostly restricted to the gastrointestinal system, whereas acidic and neutral SMases are more widely expressed and involved in physiological and pathophysiological reactions of many systems, including the cardiovascular system. In the vasculature, SMases are implicated in the regulation of vascular tone and permeability as well as in causing atherosclerotic lesions and vascular wall remodeling [13]. Interestingly, neutral SMase has been reported to induce a wide range of changes in the vascular tone, depending on the species, vessel type, and experimental conditions (Table 1.). Taken into account the large number of biologically active mediators (including ceramides, C1P, Sph, and S1P) that can be generated both extra- and intracellularly upon triggering the sphingolipid biosynthesis by neutral SMase, the diversity of vascular effects is not unexpected.

Table 1. Reported vasoactive effects of neutral SMase.

Species	Vessel	Vasoactive effects	Proposed mechanism	Ref.
Yorkshire pig	coronary artery	transient endothelium-dependent contraction followed by endothelium-dependent relaxation	vasoconstriction: prostanoid(s) vasorelaxation: NO	[14]
Sprague-Dawley rat	thoracic aorta	endothelium-independent relaxation	inhibition of protein kinase C (PKC)	[15,16]
Wistar rat	thoracic aorta	partly endothelium-independent relaxation	endothelium-mediated component is independent of NO or prostanoids; non-endothelial component is independent of PKC	[17]
Mongrel dog	basilar artery	endothelium-independent contraction	activation of VDCC and PKC	[18]
Wistar rat	pial venule (60-70 μm in diameter)	constriction and spasm	activation of VDCC, PKC, and MAP kinase	[19]
Wistar rat	thoracic aorta	endothelium-independent relaxation	inhibition of both Ca^{2+}-dependent and Ca^{2+}-independent (RhoA-/Rho ki-	[20]

			nase-mediated) contractile pathways	
Cow	coronary artery	endothelium-dependent relaxation	Ca^{2+}-independent eNOS activation, involving phosphorylation on serine 1179 and dissociation of eNOS from plasma membrane caveolae	[21]
Wistar rat	pulmonary artery	endothelium-independent contraction	activation of VDCC, PKCζ and Rho kinase	[22]
Wistar-Kyoto (WKY) and spontaneously hypertensive rat (SHR)	carotid artery	SHR: strong endothelium-dependent contraction WKY: weak endothelium-dependent contraction	vasoconstriction is mediated by PLA_2- and COX2-mediated TXA_2 release and attenuated by NO	[23-25]

NO, nitric oxide; PKC, protein kinase C; VDCC, voltage-gated calcium channel; MAP, mitogen activated protein; eNOS, endothelial NO synthase; PLA2, phospholipase A2; TXA2, thromboxane A2; COX, cyclooxygenase.

SMase enzymes are reportedly upregulated in certain cardiovascular and metabolic disorders such as type 2 diabetes mellitus (T2DM) [13,26,27]. Sphingolipids have been implicated as important regulators of inflammatory processes in diabetes [28]. Stress conditions initiate changes in sphingolipid metabolism [29], and sphingolipids have emerged as key mediators of stress responses [30,31]. Extracellular stressors induce sphingolipid synthesis and turnover, thereby 'remodeling' sphingolipid profiles and their topological distribution within cells [32]. Emerging evidence not only demonstrates profound changes in sphingolipid pools and distribution under conditions of overnutrition [33-35], but also implicates sphingolipids in mediating cell-signaling responses that precipitate pathology associated with obesity [36]. In spite of the marked alterations in the metabolism and actions of sphingolipids in diabetes and recent observations indicating that ceramide may contribute to the development of diabetic endothelial dysfunction [37], relatively little is known about the effects of sphingolipids on vascular functions in T2DM. In the present study, we analyzed the effects of SMase on vascular tone under diabetic conditions in order to elucidate the signaling mechanisms involved.

2. Results

First, we verified the general metabolic and vascular phenotype of T2DM mice tested in the present study. Db/db mice reportedly develop obesity with elevated blood glucose levels and insulin resistance [38-40]. Accordingly, the body weight increased almost 2-fold (Figure 1A), whereas blood glucose levels increased 3-fold (Figure 1B) in db/db mice as compared to non-diabetic control littermates. Furthermore, the serum phosphorylcholine level was also significantly increased in the diabetic group (Figure 1C), which is consistent with the reported enhancement of SMase activity in type 2 diabetes [13,26,27]. Vessels of db/db animals showed marked endothelial dysfunction indicated by the im-

pairment of the dose-response relationship of acetylcholine (ACh)-induced vasorelaxation after precontraction with 10 µmol/L PE (Figure 1D). The E_{max} value decreased to 50.8 ± 2.0% in diabetic vessels as compared to controls (65.8 ± 3.9%). However, there was no significant difference in the EC_{50} values (34.7 ± 16.0 nM vs. 55.7 ± 15.7 nM), indicating unchanged potency in spite of the reduced efficacy of endogenous NO upon stimulation of endothelial NOS (eNOS) by ACh. In contrast, reactivity of the vascular smooth muscle to NO remained unaltered, as neither the E_{max} (105.2 ± 1.8% vs. 103.3 ± 2.2%) nor the EC_{50} (10.7 ± 1.3 nM vs. 14.1 ± 2.0 nM) values of sodium nitroprussid (SNP)-induced vasorelaxation differed in vessels of db/db animals as compared to controls (Figure 1E). Taken together, these results confirm the T2DM-like metabolic and vascular phenotypes in db/db mice and suggest the in vivo enhancement of SMase activity as well.

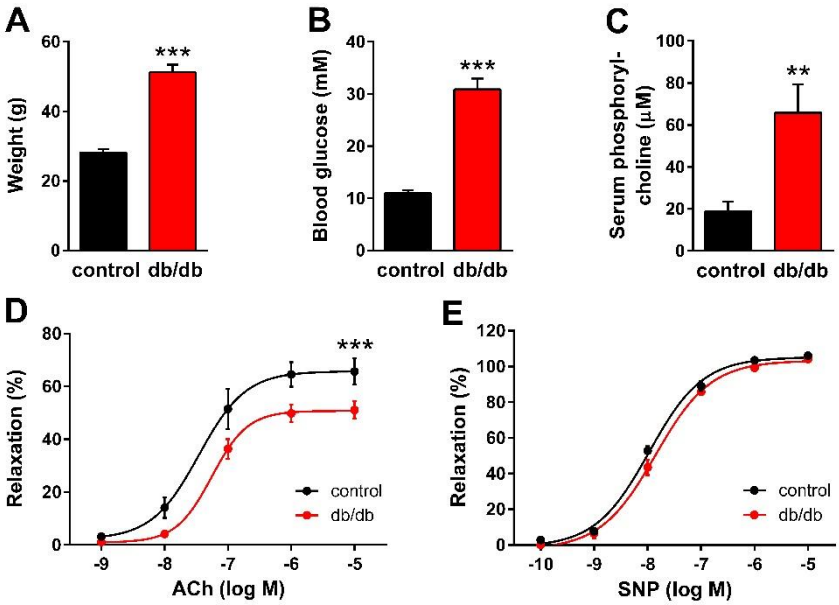

Figure 1. Manifestation of the metabolic and vascular phenotype of T2DM in db/db mice. Body weight (A), as well as non-fasting blood glucose (B) and serum phosphorylcholine levels (C) increased in db/db mice as compared to controls (**p < 0.01, ***p < 0.001 vs. control group; Student's unpaired *t*-test, n=13-22). ACh-induced relaxation diminished (D), while the reactivity of the vascular smooth muscle to sodium nitroprusside (SNP) remained unaltered (E) in vessels of db/db mice as compared to controls (mean ± SEM, ***$p < 0.001$ vs. control; dose-response curve fitted to n= 12-24).

Next, we determined the effect of nSMase on the active tone of control and db/db vessels (Figure 2A). After 10 µmol/L phenylephrine (PE)-induced precontraction, 0.2 U/mL nSMase elicited additional contraction in control vessels that reached its maximum at 7.2 min before relaxing back to the pre-SMase level by the end of the 20-min observation period. In contrast, nSMase in db/db vessels elicited completely different responses. After a marked initial relaxation elicited by 0.2 U/mL nSMase during the first 5 min, the tone of the db/db vessels remained in a relaxed state below the level of the initial tension. From the shape of the tension curve, it appeared that in addition to the overriding relaxation there was a delayed and transient constriction response, with a time course similar to that observed in control vessels, but it was unable to overcome the robust dilatation. Evaluation of the AUC (Figure 2B) and the maximal changes in the vascular

tone (Figure 2C) also supported the conclusion that there is a marked difference in the vascular effects of nSMase between control and db/db mice: contraction dominates in the former, whereas the latter is characterized by reduction of the vascular tone.

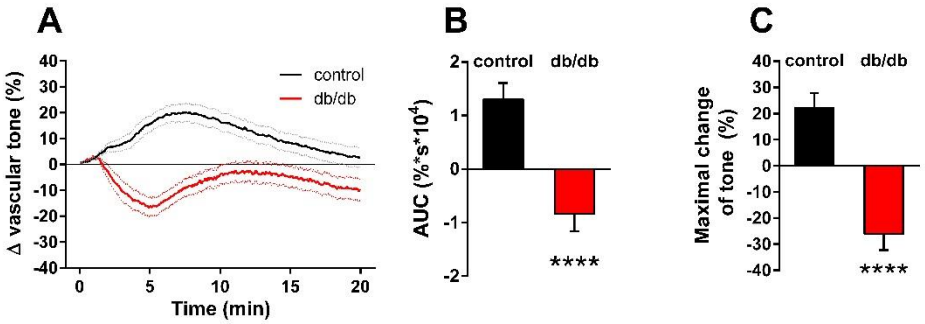

Figure 2. Effects of nSMase on the vascular tone. Application of 0.2 U/mL nSMase evoked a complex vascular effect with dominant contraction in control vessels and a more pronounced relaxation in vessels of db/db mice. Black and red lines on panel A represent average changes in tension of PE-precontracted vessels of control and db/db mice, respectively (dotted lines represent SEM). Both area under curve values (B) and maximal tension changes (C) were significantly different in vessels from db/db animals as compared to controls (mean ± SEM, Student's unpaired *t*-test, ****$p < 0.0001$ vs. control; n = 51-49).

Our next aim was to differentiate the constrictor and relaxant components of the vascular tension changes in response to nSMase. In porcine coronary arteries [14] and in carotid arteries of spontaneously hypertensive rats [23-25], prostanoids acting on TP receptors have been implicated in mediating the vasoconstrictor effect of SMase. Therefore, we hypothesized that thromboxane prostanoid (TP) receptors also mediate the nSMase-induced vasoconstriction in our murine aorta model. To test this hypothesis, the TP receptor antagonist SQ 29,548 was administered to the organ chambers 30 min prior to administration of nSMase. Blockade of TP receptors not only abolished the vasoconstriction, but also converted it to a transient vasorelaxation in control vessels (Figure 3A). The maximum of the relaxation was reached at 5.5 min after the administration of nSMase, and the vascular tone returned to the baseline after 10 min. TP receptor inhibition also markedly changed the vascular response to nSMase in the db/db group: the vasorelaxation was enhanced to more than 70% and reached its maximum at 6.5 min. After its peak, the relaxation decreased, but the vascular tone failed to return to the pre-SMase level even after 20 min. Both the AUC (Figure 3B) and the peak vasorelaxation (Figure 3C) values showed marked differences between the two experimental groups, indicating that the strongly enhanced and prolonged vasorelaxant capacity is responsible for the differences between the vasoactive effects of nSMase in db/db and control vessels. This finding was very surprising in light of the diminished ACh-induced vasorelaxation that we had observed in db/db animals (Figure 1D), and was not consistent with the large body of literary data indicating diminished endothelium-dependent vasorelaxation in T2DM..

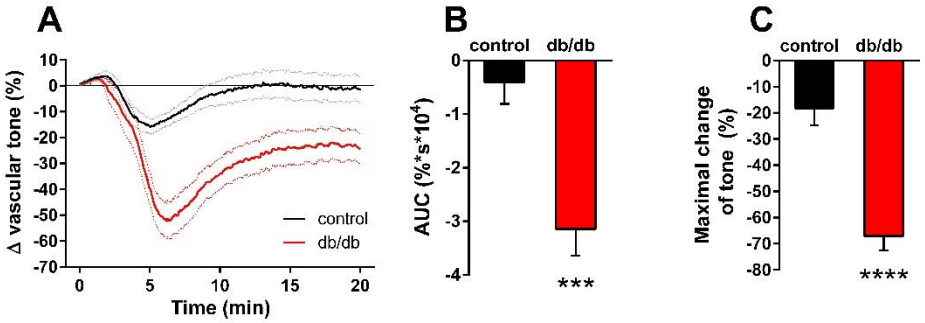

Figure 3. Effects of TP receptor blockade on nSMase-induced changes in the vascular tone. After inhibition of the TP receptor by 1 μM SQ 29,548, 0.2 U/mL nSMase relaxed both db/db and control vessels, with a significantly higher relaxation in the db/db group (A). Black and red lines in panel A represent average tension changes in PE-precontracted vessels of control and db/db mice, respectively, whereas dotted lines represent SEM. Both area under curve values (B) and maximal tension changes (C) were significantly different in vessels from db/db animals as compared to controls (mean ± SEM, Student's unpaired *t*-test, ***$p < 0.001$ vs. control; ****$p < 0.0001$ vs. control; n = 20).

Finally, we aimed to analyze the mechanism of the enhanced nSMase-induced vasorelaxation in vessels of db/db mice. Theoretically, it could be due to the enhancement of eNOS-mediated vasorelaxation or to the onset of an NO-independent mechanism. To clarify this question, the vessels were incubated with the NOS inhibitor L-NAME (100 μM) in addition to the TP receptor blocker SQ 29,548 (1 μM) for 30 min prior to 0.2 U/mL nSMase administration. L-NAME at a concentration of 100 μM abolished the vasorelaxation observed in the presence of 1 μM SQ 29,548 both in control and in db/db vessels (Figure 4A). There were no significant differences between the two groups either in the AUC (Figure 4B), or in the maximal change of tension values (Figure 4C). These results indicate that the same secondary signaling pathways – namely TP receptors and eNOS – mediate the vasoactive effects of nSMase in health and in T2DM.

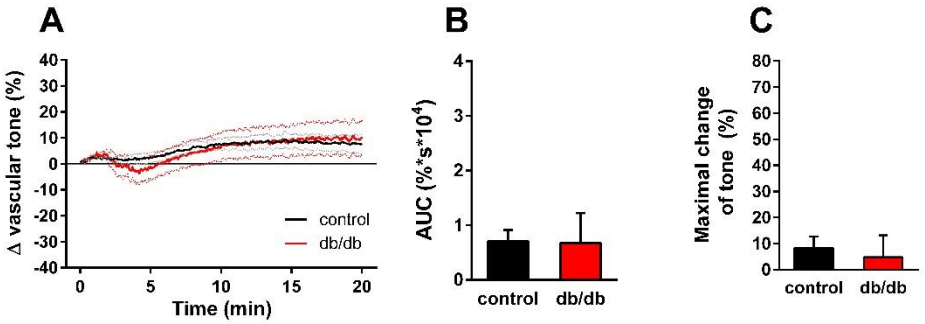

Figure 4. Effects of combined TP receptor and NOS blockade on nSMase-induced changes in vascular tone. After incubation of the vessels with 1 μM SQ 29,548 and 100 μM L-NAME for 30 min, 0.2 U/mL nSMase could no longer evoke a tension change in the thoracic aorta of control or db/db mice (A). Black and red lines in panel A represent average tension changes in PE-precontracted vessels of control and db/db mice, respectively (dotted lines represent SEM). Area under curve values (B) and maximal tension changes (C) were not different in vessels from db/db animals as compared to controls (mean ± SEM, n = 9-17).

3. Discussion

Findings of the present study indicate that nSMase-induced changes in vascular tension involve both vasoconstriction and vasorelaxation in murine vessels. Our results suggest that the former is mediated by release of prostanoids and activation of TP receptors, whereas the latter is mediated by eNOS. Surprisingly, nSMase-induced eNOS-mediated vasorelaxation is markedly enhanced in vessels of db/db mice in spite of the endothelial dysfunction indicated by the diminished vasorelaxation evoked by ACh. Therefore, nSMase appears to be able to induce enhanced NO release from endothelial cells in T2DM.

Vasoconstriction in response to SMase has been reported in a number of studies, although the mechanisms mediating this effect appear to be highly variable depending on the experimental conditions, including species, vascular region, and integrity of the endothelium (see Table 1). Release of prostanoids and consequent activation of TP receptors have been proposed in porcine coronary arteries [14] as well as in carotid arteries of spontaneously hypertensive rats [23-25]. In our study, nSMase-induced contraction was found to be TP receptor-dependent in both control and db/db mice, indicating that nSMase stimulates the release of TXA_2 from the aortic rings.

There might be at least three different sources for the SMase-induced arachidonic acid formation necessary for TXA_2 production [41]. One such possibility is that diacylglycerol (DAG) would accumulate while sphingomyelin synthase converts the newly generated ceramide back to sphingomyelin, and DAG lipases would provide arachidonic acid for the production of TXA_2 [42]. Another mechanism might relate to the observation that C1P can allosterically activate phospholipase A_2 (PLA_2) [43], which leads to arachidonic acid formation [44]. It might be important in this context that the gene encoding ceramide kinase (CERK) is upregulated in T2DM [45]. Finally, S1P has been reported recently to regulate prostanoid production in a S1P receptor-dependent manner [46].

Vasorelaxation in response to nSMase appears to be endothelial NO-dependent, as L-NAME completely abolished the decrease in vascular tone in both control and db/db vessels. Without L-NAME, the relaxation was dramatically increased in db/db-derived vascular rings. This is unexpected, because endothelial dysfunction with consequential decreased vasorelaxant capacity is considered to be a hallmark for T2DM-like conditions. A potential explanation may be related to the altered structure of the plasma membrane in T2DM [47]. Normally, sphingolmyelin (SM) represents about 10-20% of the lipids in the plasma membrane, mostly residing in the outer leaflet. However, most of these are found in the caveolae, and SMase is thought to be a regulator of lipid microdomains [48,49]. Pilarczyk and colleagues provided evidence that in db/db mice the endothelial lining of the aorta contains 10-fold larger lipid raft areas enriched in SM as compared to controls [47]. This arrangement might be related to the decreased NO-release in T2DM, as eNOS is inhibited by caveolin-1 [50], which is considered to be an important regulator of eNOS [51-53]. In our experimental setting, nSMase-induced degradation of sphingomyelin could interfere with this caveolar structure and induce the detachment of eNOS from caveolin-1, leading to high amounts of NO released from the endothelium of db/db vascular rings. This hypothesis is supported by the observations of Mogami et al. [21] indicating that SMase causes endothelium-dependent vasorelaxation

through Ca^{2+}-independent endothelial NO production in bovine aortic valves and coronary arteries. They also reported SMase-induced translocation of endothelial NOS from plasma membrane caveolae to the intracellular region. Furthermore, protein expression levels of caveolin-1 were reported to be significantly higher in the aorta of db/db mice, and this was thought to be related to the impaired aortic relaxation of C57BL/KsJ mice [54]. Still, we cannot rule out the possibility that the enhanced sphingolipid content of the membrane augments the release of sphingolipid mediators such as ceramide, and consequently enhances the ceramide-related vasorelaxation reported in non-diabetic models [15-17,20]. It has to be emphasized, though, that the ceramide-related pathway might be involved in the SMase-induced contractions as well [18,23]. Finally, the potentially increased NO-sensitivity of guanylate cyclase (sGC) [55], which could be related to the dysfunctional NO-release observed in T2DM, should also be considered, as this would sensitize sGC to NO and result in enhanced NO-mediated vasorelaxation. However, this mechanism can be excluded in our present experiments, as the SNP dose-response curve remained unchanged in db/db vessels (Figure 1E), indicating that the sensitivity of the vascular smooth muscle to NO was not upregulated.

Sphingolipid metabolism is markedly altered in T2DM and related conditions [56-60], and the observed changes in endothelial lipid rafts [47] might be a consequence of the disrupted plasma membrane lipid metabolism. On the other hand, T2DM has several characteristics that resemble a chronic inflammatory disease [61]. Cytokines that accumulate in chronic inflammation, such as tumor necrosis factor alpha (TNF-α) and interleukin 1 beta (IL-1β) can also induce marked changes in sphingolipid metabolism [6,62,63]. Our observation that the serum phosphorylcholine levels were increased in the db/db group is a strong indicator of the altered in vivo sphingolipid metabolism in our animal model and agrees with the literature.

As a limitation of our study it has to be mentioned that the characteristics of the pathophysiological conditions in the db/db mouse model differ from those of human T2DM in some aspects [64]. For example, db/db mice do not necessarily develop hypertension and may have high levels of high-density lipoprotein and a reduced tendency toward atherosclerosis [65]. Therefore, due to the more severe endothelial dysfunction, the enhancement of nSMase-induced eNOS-mediated vasorelaxation may be limited in humans with T2DM. A further limitation of our study is that we tested only one single dose of nSMase. This 0.2 U/mL dose represents the upper range used in the literature [14-18,20-23], as our aim was to evaluate the consequences of a robust activation of sphingomyelinase degradation. Further studies may aim to elucidate the exact dose-response relationship for SMase-induced vasorelaxation and vasoconstriction in db/db mice or other T2DM-related conditions, which may also help to clarify the exact molecular mechanisms involved.

4. Materials and Methods

All procedures were carried out according to the guidelines of the Hungarian Law of Animal Protection (28/1998) and were approved by the National Scientific Ethical Committee on Animal Experimentation (PEI/001/2706-13/2014).

4.1. Animals and general procedures

The BKS db diabetic mouse strain (JAX stock #000642) was obtained from The Jackson Laboratory (Bar Harbor, ME, USA) and has been maintained in our animal facility by mating repulsion double heterozygotes (Dock7^{m} +/+ Lepr^{db}). Littermate adult male diabetic (Lepr^{db}/Lepr^{db}, referred to as db/db) and misty (Dock7^{m}/Dock7^{m}, referred to as control) mice were selected for experiments. Animals were weighed, and blood samples were collected by cardiac puncture followed by transcardial perfusion with 10 mL heparinized (10 IU/mL) Krebs solution under deep ether anesthesia as described previously [66]. Nonfasting blood glucose was measured by Dcont IDEÁL biosensor type blood glucose meter (77 Elektronika Kft.; Budapest, Hungary). In some experiments, additional blood samples were collected, allowed to clot for 30 min at room temperature, and centrifuged at 2000 x g for 15 min at 4 °C. Serum was snap frozen for later phosphorylcholine assay, which was based on the method described by Hojjati and Jiang [67] using a commercially available kit (Item № 10009928, Cayman Chemical; Ann Arbor, MI, US).

4.2. Myography

The thoracic aorta was removed and cleaned of fat and connective tissue under a dissection microscope (M3Z, Wild Heerbrugg AG; Gais, Switzerland) and immersed in a Krebs solution of the following composition (mmol/L): 119 NaCl, 4.7 KCl, 1.2 KH_2PO_4, 2.5 $CaCl_2 \cdot 2\ H_2O$, 1.2 $MgSO_4 \cdot 7\ H_2O$, 20 $NaHCO_3$, 0.03 EDTA, and 10 glucose at room temperature and pH 7.4. Vessels were cut into ~3 mm-long segments and mounted on stainless steel vessel holders (200 μm in diameter) in a conventional myograph setup (610 M multiwire myograph system; Danish Myo Technology A/S; Aarhus, Denmark). Special care was taken to preserve the endothelium.

Wells of the myographs were filled with 8 mL Krebs solution aerated with carbogen. The vessels were allowed a 30-min resting period, during which the bath solution was warmed to 37 °C and the passive tension was adjusted to 15 mN, which was determined to be optimal in a previous study [66]. Subsequently, the tissues were exposed to 124 mmol/L K^+ Krebs solution (made by isomolar replacement of Na^+ by K^+) for 1 min, followed by several washes with normal Krebs solution. Reactivity of the smooth muscle was tested by a contraction evoked by 10 μmol/L PE, and reactivity of the endothelium was tested by following the PE-evoked contraction with administration of 0.1 μmol/L ACh. After repeated washing, during which the vascular tension returned to the resting level, the segments were exposed to 124 mmol/L K^+ Krebs solution for 3 min in order to elicit a reference maximal contraction. Subsequently, after a 30-min washout, increasing concentrations of PE (0.1 nmol/L to 10 μmol/L) and ACh (1 nmol/L to 10 μmol/L) were administered to determine the reactivity of the smooth muscle and the endothelium, respectively. Following a 30-min resting period, the vessels were precontracted to 70-90% of the reference contraction by an appropriate concentration of PE; and after contraction had stabilized, the effects of 0.2 U/mL nSMase (SMase from *B. cereus*, Sigma-Aldrich; St. Louis, MO, USA) were investigated for 20 min. Bacterial SMase functions in neutral pH, and is reportedly a useful tool for mimicking the biological effects of activation of cellular SMase [68,69]. In some experiments, the selective TP receptor antagonist

SQ-29548 (1 μM) with or without the nitric oxide synthase (NOS) inhibitor L-NAME (100 μM) was applied to the baths 30 min prior to administration of nSMase. Finally, to test the sensitivity of the smooth muscle to NO, SNP (0.1 nmol/L to 10 μmol/L) was administered after a stable precontraction elicited by 1 μmol/L PE.

4.3. Data Analysis

An MP100 system and AcqKnowledge 3.72 software from Biopac System Inc. (Goleta, CA, USA) were used to record and analyze changes in the vascular tone. All data are presented as mean ± SE, and *n* indicates the number of vascular segments tested in myography experiments or the number of animals tested in the case of body weight, blood glucose, and serum phosphorylcholine levels. Maximal changes of the vascular tone were calculated as a percentage of pre-contraction. To evaluate the temporal pattern of nSMase-induced vasoactive responses, individual curves were constructed and averaged, showing the changes in vascular tone for 20 min after the application of nSMase. Area under curve (AUC) values were calculated from the individual experiments for quantification of the overall vasoactive effect. The statistical analysis was performed using the GraphPad Prism software v.6.07 from GraphPad Software Inc. (La Jolla, CA, USA). Student's unpaired *t*test was applied when comparing two variables, and a p value of less than 0.05 was considered to be statistically significant. Effects of cumulative doses of PE and ACh were evaluated by dose-response curve fitting for determination of E_{max} and EC_{50} values.

4.4. Reagents

All reagents in this study, including nSMase, were purchased from Sigma-Aldrich (St. Louis, MO, USA) except SQ-29548, which was from Santa Cruz Biotechnology (Dallas, TX, USA).

5. Conclusions

Administration of nSMase induces TP receptor-mediated vasoconstriction and eNOS-mediated vasorelaxation in murine vessels. In spite of endothelial dysfunction in db/db mice, the vasorelaxant effect of nSMase is markedly augmented. SMase-mediated disruption of SM in endothelial lipid rafts might represent a possible mechanism responsible for enhanced NO generation in T2DM. An intriguing interpretation of our finding is that retraction of eNOS in sphingomyelin-rich microdomains of the endothelial plasma membrane could contribute significantly to the development of vascular dysfunction in T2DM.

Author Contributions: Conceptualization, É.R., L.K., G.T. and Z.B.; methodology, É.R. and Z.B.; validation, K.L., G.T. and Z.B.; investigation, É.R., R.C.P. A.P., Z.S. and D.K.; resources, Z.B.; data curation, É.R, R.C.P. A.J., A.P., Z.S. and D.K..; writing—original draft preparation, É.R., A.J., L.K., K.L., G.T and Z.B..; visualization, É.R and A.J.; supervision, L.K., K.L., G.T and Z.B.; project administration, Z.B.; funding acquisition, É.R. and Z.B.

Funding: This research was funded by the Hungarian National Research, Development, and Innovation Office (OTKA K-112964, K-125174, K-139230 and PD-132851) and by the Ministry of Innovation and Technology of Hungary from the NRDI Fund (2020-1.1.6-JÖVŐ-2021-00010, 2020-1.1.6-JÖVŐ-2021-00013 and TKP2021-EGA-25).

Institutional Review Board Statement: The animal experiments were carried out according to the guidelines of the Hungarian Law of Animal Protection (28/1998) and were approved by the National Scientific Ethical Committee on Animal Experimentation (PEI/001/2706-13/2014).

Data Availability Statement: The data presented in this study are available in Supplemetal file.

Acknowledgments: The authors are grateful to Margit Kerék for expert technical assistance and to Dr. Erzsébet Fejes for critically reading the manuscript.

Conflicts of Interest: The authors declare no conflict of interest. The funders had no role in the design of the study; in the collection, analyses, or interpretation of data; in the writing of the manuscript; or in the decision to publish the results.

References

1. Peters, S.L.; Alewijnse, A.E. Sphingosine-1-phosphate signaling in the cardiovascular system. *Curr Opin Pharmacol* **2007**, *7*, 186-192, doi:10.1016/j.coph.2006.09.008.
2. Igarashi, J.; Michel, T. Sphingosine-1-phosphate and modulation of vascular tone. *Cardiovasc Res* **2009**, *82*, 212-220, doi:10.1093/cvr/cvp064.
3. Kerage, D.; Brindley, D.N.; Hemmings, D.G. Review: novel insights into the regulation of vascular tone by sphingosine 1-phosphate. *Placenta* **2014**, *35 Suppl*, S86-92, doi:10.1016/j.placenta.2013.12.006.
4. Proia, R.L.; Hla, T. Emerging biology of sphingosine-1-phosphate: its role in pathogenesis and therapy. *J Clin Invest* **2015**, *125*, 1379-1387, doi:10.1172/JCI76369.
5. Hemmings, D.G. Signal transduction underlying the vascular effects of sphingosine 1-phosphate and sphingosylphosphorylcholine. *Naunyn Schmiedebergs Arch Pharmacol* **2006**, *373*, 18-29, doi:10.1007/s00210-006-0046-5.
6. De Palma, C.; Meacci, E.; Perrotta, C.; Bruni, P.; Clementi, E. Endothelial nitric oxide synthase activation by tumor necrosis factor alpha through neutral sphingomyelinase 2, sphingosine kinase 1, and sphingosine 1 phosphate receptors: a novel pathway relevant to the pathophysiology of endothelium. *Arterioscler Thromb Vasc Biol* **2006**, *26*, 99-105, doi:10.1161/01.ATV.0000194074.59584.42.
7. Fyrst, H.; Saba, J.D. An update on sphingosine-1-phosphate and other sphingolipid mediators. *Nature chemical biology* **2010**, *6*, 489-497, doi:10.1038/nchembio.392.
8. Meyer zu Heringdorf, D.; Jakobs, K.H. Lysophospholipid receptors: signalling, pharmacology and regulation by lysophospholipid metabolism. *Biochim Biophys Acta* **2007**, *1768*, 923-940, doi:10.1016/j.bbamem.2006.09.026.
9. Strub, G.M.; Maceyka, M.; Hait, N.C.; Milstien, S.; Spiegel, S. Extracellular and intracellular actions of sphingosine-1-phosphate. *Advances in experimental medicine and biology* **2010**, *688*, 141-155.
10. Hla, T.; Dannenberg, A.J. Sphingolipid signaling in metabolic disorders. *Cell Metab* **2012**, *16*, 420-434, doi:10.1016/j.cmet.2012.06.017.
11. Ernst, A.M.; Brugger, B. Sphingolipids as modulators of membrane proteins. *Biochim Biophys Acta* **2014**, *1841*, 665-670, doi:10.1016/j.bbalip.2013.10.016.
12. Adada, M.; Luberto, C.; Canals, D. Inhibitors of the sphingomyelin cycle: sphingomyelin synthases and sphingomyelinases. *Chemistry and physics of lipids* **2016**, *197*, 45-59, doi:10.1016/j.chemphyslip.2015.07.008.
13. Pavoine, C.; Pecker, F. Sphingomyelinases: their regulation and roles in cardiovascular pathophysiology. *Cardiovasc Res* **2009**, *82*, 175-183, doi:10.1093/cvr/cvp030.
14. Murohara, T.; Kugiyama, K.; Ohgushi, M.; Sugiyama, S.; Ohta, Y.; Yasue, H. Effects of sphingomyelinase and sphingosine on arterial vasomotor regulation. *J Lipid Res* **1996**, *37*, 1601-1608.
15. Johns, D.G.; Jin, J.S.; Wilde, D.W.; Webb, R.C. Ceramide-induced vasorelaxation: An inhibitory action on protein kinase C. *General pharmacology* **1999**, *33*, 415-421.
16. Johns, D.G.; Osborn, H.; Webb, R.C. Ceramide: a novel cell signaling mechanism for vasodilation. *Biochemical and biophysical research communications* **1997**, *237*, 95-97, doi:10.1006/bbrc.1997.7084.
17. Zheng, T.; Li, W.; Wang, J.; Altura, B.T.; Altura, B.M. Effects of neutral sphingomyelinase on phenylephrine-induced vasoconstriction and Ca(2+) mobilization in rat aortic smooth muscle. *European journal of pharmacology* **2000**, *391*, 127-135.
18. Zheng, T.; Li, W.; Wang, J.; Altura, B.T.; Altura, B.M. Sphingomyelinase and ceramide analogs induce contraction and rises in [Ca(2+)](i) in canine cerebral vascular muscle. *Am J Physiol Heart Circ Physiol* **2000**, *278*, H1421-1428.
19. Altura, B.M.; Gebrewold, A.; Zheng, T.; Altura, B.T. Sphingomyelinase and ceramide analogs induce vasoconstriction and leukocyte-endothelial interactions in cerebral venules in the intact rat brain: Insight into mechanisms and possible relation to brain injury and stroke. *Brain research bulletin* **2002**, *58*, 271-278.
20. Jang, G.J.; Ahn, D.S.; Cho, Y.E.; Morgan, K.G.; Lee, Y.H. C2-ceramide induces vasodilation in phenylephrine-induced pre-contracted rat thoracic aorta: role of RhoA/Rho-kinase and intracellular Ca2+ concentration. *Naunyn Schmiedebergs Arch Pharmacol* **2005**, *372*, 242-250, doi:10.1007/s00210-005-0008-3.
21. Mogami, K.; Kishi, H.; Kobayashi, S. Sphingomyelinase causes endothelium-dependent vasorelaxation through endothelial nitric oxide production without cytosolic Ca(2+) elevation. *FEBS Lett* **2005**, *579*, 393-397, doi:10.1016/j.febslet.2004.11.100.

22. Cogolludo, A.; Moreno, L.; Frazziano, G.; Moral-Sanz, J.; Menendez, C.; Castaneda, J.; Gonzalez, C.; Villamor, E.; Perez-Vizcaino, F. Activation of neutral sphingomyelinase is involved in acute hypoxic pulmonary vasoconstriction. *Cardiovasc Res* **2009**, *82*, 296-302, doi:10.1093/cvr/cvn349.
23. Spijkers, L.J.; van den Akker, R.F.; Janssen, B.J.; Debets, J.J.; De Mey, J.G.; Stroes, E.S.; van den Born, B.J.; Wijesinghe, D.S.; Chalfant, C.E.; MacAleese, L.; et al. Hypertension is associated with marked alterations in sphingolipid biology: a potential role for ceramide. *PLoS One* **2011**, *6*, e21817, doi:10.1371/journal.pone.0021817.
24. Spijkers, L.J.; Janssen, B.J.; Nelissen, J.; Meens, M.J.; Wijesinghe, D.; Chalfant, C.E.; De Mey, J.G.; Alewijnse, A.E.; Peters, S.L. Antihypertensive treatment differentially affects vascular sphingolipid biology in spontaneously hypertensive rats. *PLoS One* **2011**, *6*, e29222, doi:10.1371/journal.pone.0029222.
25. van den Elsen, L.W.; Spijkers, L.J.; van den Akker, R.F.; van Winssen, A.M.; Balvers, M.; Wijesinghe, D.S.; Chalfant, C.E.; Garssen, J.; Willemsen, L.E.; Alewijnse, A.E.; et al. Dietary fish oil improves endothelial function and lowers blood pressure via suppression of sphingolipid-mediated contractions in spontaneously hypertensive rats. *Journal of hypertension* **2014**, *32*, 1050-1058; discussion 1058, doi:10.1097/HJH.0000000000000131.
26. Shamseddine, A.A.; Airola, M.V.; Hannun, Y.A. Roles and regulation of neutral sphingomyelinase-2 in cellular and pathological processes. *Advances in biological regulation* **2015**, *57*, 24-41, doi:10.1016/j.jbior.2014.10.002.
27. Russo, S.B.; Ross, J.S.; Cowart, L.A. Sphingolipids in obesity, type 2 diabetes, and metabolic disease. *Handb Exp Pharmacol* **2013**, 373-401, doi:10.1007/978-3-7091-1511-4_19.
28. Cowart, L.A. Sphingolipids: players in the pathology of metabolic disease. *Trends in endocrinology and metabolism* **2009**, *20*, 34-42, doi:10.1016/j.tem.2008.09.004.
29. Hannun, Y.A.; Obeid, L.M. The ceramide-centric universe of lipid-mediated cell regulation: stress encounters of the lipid kind. *J Biol Chem* **2002**, *277*, 25847-25850, doi:10.1074/jbc.R200008200.
30. Sawai, H.; Hannun, Y.A. Ceramide and sphingomyelinases in the regulation of stress responses. *Chemistry and physics of lipids* **1999**, *102*, 141-147.
31. Hannun, Y.A.; Luberto, C. Ceramide in the eukaryotic stress response. *Trends in cell biology* **2000**, *10*, 73-80.
32. van Meer, G.; Holthuis, J.C. Sphingolipid transport in eukaryotic cells. *Biochimica et biophysica acta* **2000**, *1486*, 145-170.
33. Holland, W.L.; Summers, S.A. Sphingolipids, insulin resistance, and metabolic disease: new insights from in vivo manipulation of sphingolipid metabolism. *Endocrine reviews* **2008**, *29*, 381-402, doi:10.1210/er.2007-0025.
34. Unger, R.H.; Orci, L. Lipoapoptosis: its mechanism and its diseases. *Biochim Biophys Acta* **2002**, *1585*, 202-212.
35. Boden, G. Pathogenesis of type 2 diabetes. Insulin resistance. *Endocrinology and metabolism clinics of North America* **2001**, *30*, 801-815, v.
36. Samad, F. Contribution of sphingolipids to the pathogenesis of obesity. *Future lipidology* **2007**, *2*, 625-639, doi:10.2217/17460875.2.6.625.
37. Symons, J.D.; Abel, E.D. Lipotoxicity contributes to endothelial dysfunction: a focus on the contribution from ceramide. *Reviews in endocrine and metabolic disorders* **2013**, *14*, 59-68, doi:10.1007/s11154-012-9235-3.
38. Aasum, E.; Hafstad, A.D.; Severson, D.L.; Larsen, T.S. Age-dependent changes in metabolism, contractile function, and ischemic sensitivity in hearts from db/db mice. *Diabetes* **2003**, *52*, 434-441.
39. Coleman, D.L. Obese and diabetes: two mutant genes causing diabetes-obesity syndromes in mice. *Diabetologia* **1978**, *14*, 141-148.
40. Do, O.H.; Low, J.T.; Gaisano, H.Y.; Thorn, P. The secretory deficit in islets from db/db mice is mainly due to a loss of responding beta cells. *Diabetologia* **2014**, *57*, 1400-1409, doi:10.1007/s00125-014-3226-8.
41. Ramadan, F.M.; Upchurch, G.R., Jr.; Keagy, B.A.; Johnson, G., Jr. Endothelial cell thromboxane production and its inhibition by a calcium-channel blocker. *The Annals of thoracic surgery* **1990**, *49*, 916-919.
42. Epand, R.M.; So, V.; Jennings, W.; Khadka, B.; Gupta, R.S.; Lemaire, M. Diacylglycerol Kinase-epsilon: Properties and Biological Roles. *Frontiers in cell and developmental biology* **2016**, *4*, 112, doi:10.3389/fcell.2016.00112.
43. Subramanian, P.; Vora, M.; Gentile, L.B.; Stahelin, R.V.; Chalfant, C.E. Anionic lipids activate group IVA cytosolic phospholipase A2 via distinct and separate mechanisms. *J Lipid Res* **2007**, *48*, 2701-2708, doi:10.1194/jlr.M700356-JLR200.
44. Pettus, B.J.; Bielawska, A.; Spiegel, S.; Roddy, P.; Hannun, Y.A.; Chalfant, C.E. Ceramide kinase mediates cytokine- and calcium ionophore-induced arachidonic acid release. *J Biol Chem* **2003**, *278*, 38206-38213, doi:10.1074/jbc.M304816200.
45. Mitsutake, S.; Date, T.; Yokota, H.; Sugiura, M.; Kohama, T.; Igarashi, Y. Ceramide kinase deficiency improves diet-induced obesity and insulin resistance. *FEBS Lett* **2012**, *586*, 1300-1305, doi:10.1016/j.febslet.2012.03.032.
46. Machida, T.; Matamura, R.; Iizuka, K.; Hirafuji, M. Cellular function and signaling pathways of vascular smooth muscle cells modulated by sphingosine 1-phosphate. *J Pharmacol Sci* **2016**, *132*, 211-217, doi:10.1016/j.jphs.2016.05.010.
47. Pilarczyk, M.; Mateuszuk, L.; Rygula, A.; Kepczynski, M.; Chlopicki, S.; Baranska, M.; Kaczor, A. Endothelium in spots--high-content imaging of lipid rafts clusters in db/db mice. *PLoS One* **2014**, *9*, e106065, doi:10.1371/journal.pone.0106065.
48. Mitsutake, S.; Zama, K.; Yokota, H.; Yoshida, T.; Tanaka, M.; Mitsui, M.; Ikawa, M.; Okabe, M.; Tanaka, Y.; Yamashita, T.; et al. Dynamic modification of sphingomyelin in lipid microdomains controls development of obesity, fatty liver, and type 2 diabetes. *J Biol Chem* **2011**, *286*, 28544-28555, doi:10.1074/jbc.M111.255646.
49. Romiti, E.; Meacci, E.; Tanzi, G.; Becciolini, L.; Mitsutake, S.; Farnararo, M.; Ito, M.; Bruni, P. Localization of neutral ceramidase in caveolin-enriched light membranes of murine endothelial cells. *FEBS Lett* **2001**, *506*, 163-168.

50. Jasmin, J.F., Frank, P.G., Lisanti, M.P. Caveolins and caveolae: roles in signaling and disease mechanism. *Advances in experimental medicine and biology, New York: Springer Science+Business Media, LCC.* **2012**, 3–13.
51. Garcia-Cardena, G.; Martasek, P.; Masters, B.S.; Skidd, P.M.; Couet, J.; Li, S.; Lisanti, M.P.; Sessa, W.C. Dissecting the interaction between nitric oxide synthase (NOS) and caveolin. Functional significance of the nos caveolin binding domain in vivo. *J Biol Chem* **1997**, *272*, 25437-25440.
52. Frank, P.G.; Woodman, S.E.; Park, D.S.; Lisanti, M.P. Caveolin, caveolae, and endothelial cell function. *Arterioscler Thromb Vasc Biol* **2003**, *23*, 1161-1168, doi:10.1161/01.ATV.0000070546.16946.3A.
53. Shaul, P.W. Regulation of endothelial nitric oxide synthase: location, location, location. *Annual review of physiology* **2002**, *64*, 749-774, doi:10.1146/annurev.physiol.64.081501.155952.
54. Lam, T.Y.; Seto, S.W.; Lau, Y.M.; Au, L.S.; Kwan, Y.W.; Ngai, S.M.; Tsui, K.W. Impairment of the vascular relaxation and differential expression of caveolin-1 of the aorta of diabetic +db/+db mice. *Eur J Pharmacol* **2006**, *546*, 134-141, doi:10.1016/j.ejphar.2006.07.003.
55. Miller, M.A.; Morgan, R.J.; Thompson, C.S.; Mikhailidis, D.P.; Jeremy, J.Y. Adenylate and guanylate cyclase activity in the penis and aorta of the diabetic rat: an in vitro study. *British journal of urology* **1994**, *74*, 106-111.
56. Samad, F.; Hester, K.D.; Yang, G.; Hannun, Y.A.; Bielawski, J. Altered adipose and plasma sphingolipid metabolism in obesity: a potential mechanism for cardiovascular and metabolic risk. *Diabetes* **2006**, *55*, 2579-2587, doi:10.2337/db06-0330.
57. Arora, T.; Velagapudi, V.; Pournaras, D.J.; Welbourn, R.; le Roux, C.W.; Oresic, M.; Backhed, F. Roux-en-Y gastric bypass surgery induces early plasma metabolomic and lipidomic alterations in humans associated with diabetes remission. *PLoS One* **2015**, *10*, e0126401, doi:10.1371/journal.pone.0126401.
58. Fox, T.E.; Bewley, M.C.; Unrath, K.A.; Pedersen, M.M.; Anderson, R.E.; Jung, D.Y.; Jefferson, L.S.; Kim, J.K.; Bronson, S.K.; Flanagan, J.M.; et al. Circulating sphingolipid biomarkers in models of type 1 diabetes. *J Lipid Res* **2011**, *52*, 509-517, doi:10.1194/jlr.M010595.
59. Gorska, M.; Baranczuk, E.; Dobrzyn, A. Secretory Zn2+-dependent sphingomyelinase activity in the serum of patients with type 2 diabetes is elevated. *Hormone and metabolic research = Hormon- und Stoffwechselforschung = Hormones et metabolisme* **2003**, *35*, 506-507, doi:10.1055/s-2003-41810.
60. Gorska, M.; Dobrzyn, A.; Baranowski, M. Concentrations of sphingosine and sphinganine in plasma of patients with type 2 diabetes. *Medical science monitor : international medical journal of experimental and clinical research* **2005**, *11*, CR35-38.
61. Donath, M.Y.; Shoelson, S.E. Type 2 diabetes as an inflammatory disease. *Nature reviews. Immunology* **2011**, *11*, 98-107, doi:10.1038/nri2925.
62. Dressler, K.A.; Mathias, S.; Kolesnick, R.N. Tumor necrosis factor-alpha activates the sphingomyelin signal transduction pathway in a cell-free system. *Science* **1992**, *255*, 1715-1718.
63. Wiegmann, K.; Schutze, S.; Machleidt, T.; Witte, D.; Kronke, M. Functional dichotomy of neutral and acidic sphingomyelinases in tumor necrosis factor signaling. *Cell* **1994**, *78*, 1005-1015.
64. Wang, B.; Chandrasekera, P.C.; Pippin, J.J. Leptin- and leptin receptor-deficient rodent models: relevance for human type 2 diabetes. *Current diabetes reviews* **2014**, *10*, 131-145.
65. Cohen, M.P.; Clements, R.S.; Hud, E.; Cohen, J.A.; Ziyadeh, F.N. Evolution of renal function abnormalities in the db/db mouse that parallels the development of human diabetic nephropathy. *Experimental nephrology* **1996**, *4*, 166-171.
66. Horvath, B.; Orsy, P.; Benyo, Z. Endothelial NOS-mediated relaxations of isolated thoracic aorta of the C57BL/6J mouse: a methodological study. *J Cardiovasc Pharmacol* **2005**, *45*, 225-231, doi:10.1097/01.fjc.0000154377.90069.b9.
67. Hojjati, M.R.; Jiang, X.C. Rapid, specific, and sensitive measurements of plasma sphingomyelin and phosphatidylcholine. *J Lipid Res* **2006**, *47*, 673-676, doi:10.1194/jlr.D500040-JLR200.
68. Raines, M.A.; Kolesnick, R.N.; Golde, D.W. Sphingomyelinase and ceramide activate mitogen-activated protein kinase in myeloid HL-60 cells. *J Biol Chem* **1993**, *268*, 14572-14575.
69. Linardic, C.M.; Hannun, Y.A. Identification of a distinct pool of sphingomyelin involved in the sphingomyelin cycle. *J Biol Chem* **1994**, *269*, 23530-23537.